

Supporting Information

# Heterodinuclear Complexes Featuring Zn(II) and M = Al(III), Ga(III) or In(III) for Cyclohexene Oxide and CO<sub>2</sub> Copolymerisation

Arron C. Deacy, Christopher B. Durr and Charlotte K. Williams\*

Department of Chemistry, University of Oxford, Oxford, OX1 3TA, UK

Part A: Characterization

Part B: X – ray crystallographic data

Figure S1: <sup>1</sup> H NMR of <b>1</b> ( <i>d</i> <sub>2</sub> -TCE, 403 K).....	3
Figure S2: <sup>13</sup> C NMR of <b>1</b> ( <i>d</i> <sub>2</sub> -TCE, 403 K).....	3
Figure S3: <sup>1</sup> H NMR of <b>2</b> ( <i>d</i> <sub>3</sub> -MeCN, 298 K).....	4
Figure S4: 2D HSQC NMR of <b>2</b> ( <i>d</i> <sub>8</sub> -THF, 298 K).....	4
Figure S5: 2D COSY NMR of <b>2</b> ( <i>d</i> <sub>8</sub> -THF, 298 K).....	5
Figure S6: <sup>13</sup> C NMR of <b>2</b> ( <i>d</i> <sub>3</sub> -MeCN, 298 K).....	5
Figure S7: <sup>1</sup> H NMR of <b>3</b> ( <i>d</i> <sub>3</sub> -MeCN, 298 K).....	6
Figure S8: 2D HSQC NMR of <b>3</b> ( <i>d</i> <sub>3</sub> -MeCN, 298 K).....	6
Figure S9: 2D COSY NMR of <b>3</b> ( <i>d</i> <sub>3</sub> -MeCN, 298 K).....	7
Figure S10: <sup>13</sup> C NMR of <b>3</b> ( <i>d</i> <sub>3</sub> -MeCN, 298 K).....	7
Figure S11: 2D DOSY NMR of <b>3</b> ( <i>d</i> <sub>3</sub> -MeCN, 298 K).....	8
Figure S12: <sup>1</sup> H NMR of <b>4</b> ( <i>d</i> <sub>8</sub> -THF, 298 K).....	8
Figure S13: 2D HSQC NMR of <b>4</b> ( <i>d</i> <sub>8</sub> -THF, 298 K).....	9
Figure S14: 2D COSY NMR of <b>4</b> ( <i>d</i> <sub>8</sub> -THF, 298 K).....	9
Figure S15: <sup>13</sup> C NMR of <b>4</b> ( <i>d</i> <sub>8</sub> -THF, 298 K).....	10
Figure S16: 2D DOSY NMR of <b>4</b> ( <i>d</i> <sub>8</sub> -THF, 298 K).....	10
Figure S17: <sup>1</sup> H NMR spectrum of complex <b>5</b> ( <i>d</i> <sub>8</sub> -THF, 298 K).....	11
Figure S18: HSQC NMR of complex <b>5</b> ( <i>d</i> <sub>8</sub> -THF, 298 K).....	11
Figure S19: <sup>11</sup> B NMR of complex <b>5</b> ( <i>d</i> <sub>8</sub> -THF, 298 K).....	12
Figure S20: <sup>13</sup> C NMR of complex <b>5</b> ( <i>d</i> <sub>8</sub> -THF, 298 K).....	12
Figure S21: <sup>19</sup> F NMR of complex <b>5</b> ( <i>d</i> <sub>8</sub> -THF, 298 K).....	13
Figure S22: <sup>1</sup> H NMR spectrum of complex <b>6</b> ( <i>d</i> <sub>4</sub> -MeOD, 298 K).....	13
Figure S23: HSQC NMR of complex <b>6</b> ( <i>d</i> <sub>4</sub> -MeOD, 298 K).....	14
Figure S24: <sup>13</sup> C NMR of complex <b>6</b> ( <i>d</i> <sub>4</sub> -MeOD, 298 K).....	14
Figure S25: 2D DOSY NMR of complex <b>6</b> ( <i>d</i> <sub>4</sub> -MeOD, 298 K).....	15
Figure S26: MALDI – ToF mass spectrum of <b>1</b> .....	15
Figure S27: MALDI – ToF mass spectrum of <b>2</b> .....	16
Figure S28: MALDI – ToF mass spectrum of <b>3</b> .....	16
Figure S29: MALDI – ToF mass spectrum of <b>4</b> .....	17
Figure S30: ORTEP representation of the molecular structure of <b>1</b> with disorder and hydrogen atoms (excluding NH) omitted for clarity with thermal ellipsoids represented at 40 % probability.....	18

Figure S31: ORTEP representation of the molecular structure of <b>2</b> with disorder and hydrogen atoms (excluding NH) omitted for clarity with thermal ellipsoids represented at 40 % probability.....	19
Figure S32: ORTEP representation of the molecular structure of <b>3</b> with disorder and hydrogen atoms (excluding NH) omitted for clarity with thermal ellipsoids represented at 40 % probability.....	20
Figure S33: ORTEP representation of the molecular structure of <b>4</b> with disorder and hydrogen atoms (excluding NH) omitted for clarity with thermal ellipsoids represented at 40 % probability.....	21
Figure S34: Connectivity data of the molecular structure of <b>6</b> with disorder and hydrogen atoms (excluding NH) omitted for clarity with thermal ellipsoids represented at 40 % probability.....	22
Figure S35: Molecular structures of other Group 13 active for CO <sub>2</sub> /CHO ROCOP. ....	23
Figure S36: Illustration of the catalytic cycle to polycarbonate formation, along with side reactions resulting in cyclic carbonate and polyether linkages. ....	24
Figure S37: Complex <b>2</b> heated to 100 °C in THF for 3 days.....	24
Figure S38 : Complex <b>3</b> heated to 100 °C in THF for 3 days.....	25
Figure S39: Complex <b>4</b> heated to 100 °C in THF for 3 days.....	25
Figure S40: Representative <sup>1</sup> H NMR of crude polymerisation mixture containing polycarbonate (4.65 ppm) trans-cyclic carbonate (4.00 ppm) and polyether (3.45 ppm) in CDCl <sub>3</sub> at 298 K. ....	26
Figure S41: GPC of crude reaction samples reported in Table 1 for a) Entry 1, b) Entry 4, c) Entry 5 and d) Entry 6.....	27

## Part A: Characterisation Data

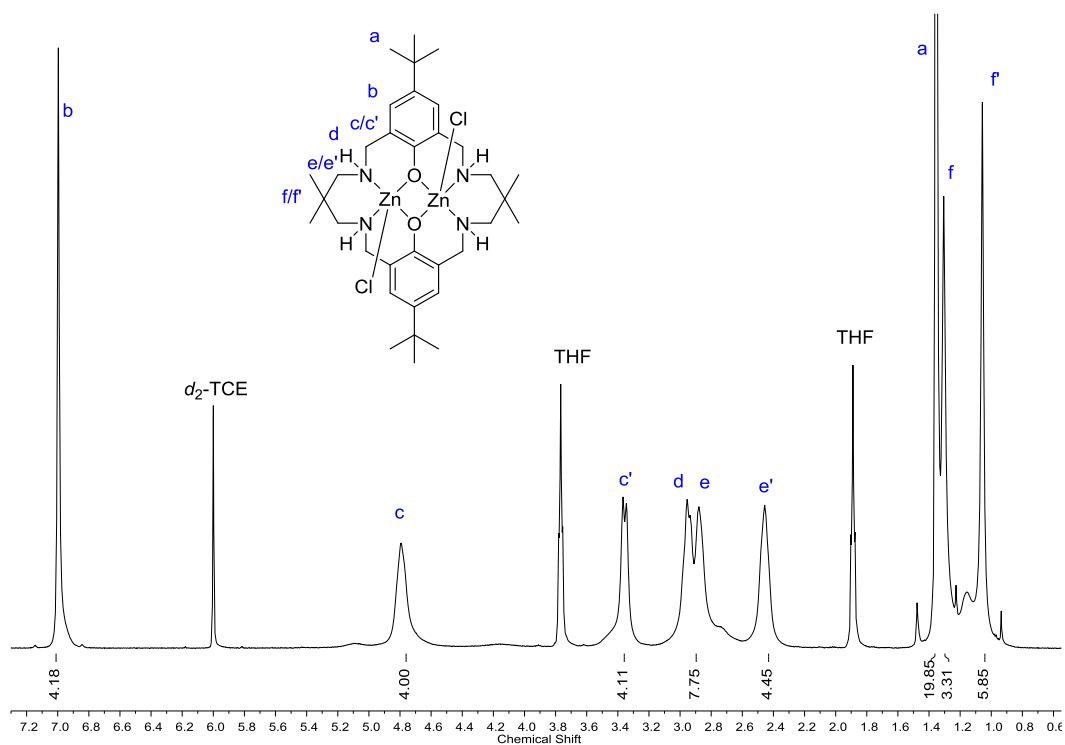


Figure S1:  $^1\text{H}$  NMR of **1** ( $d_2$ -TCE, 403 K)

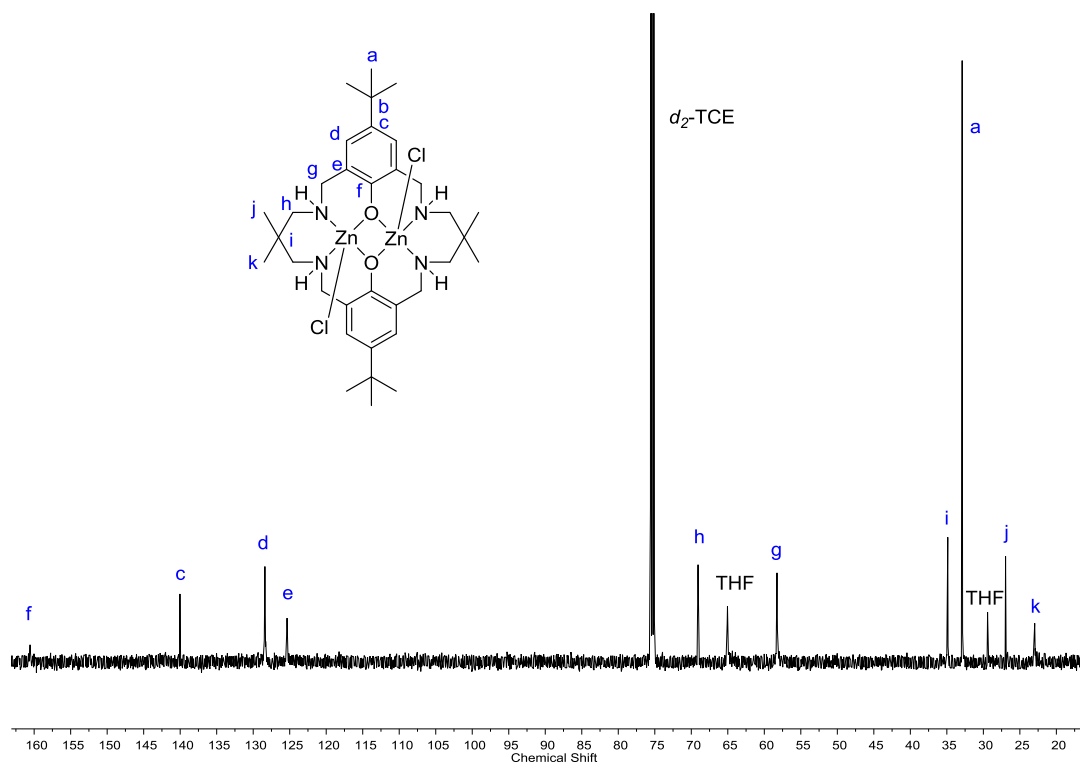
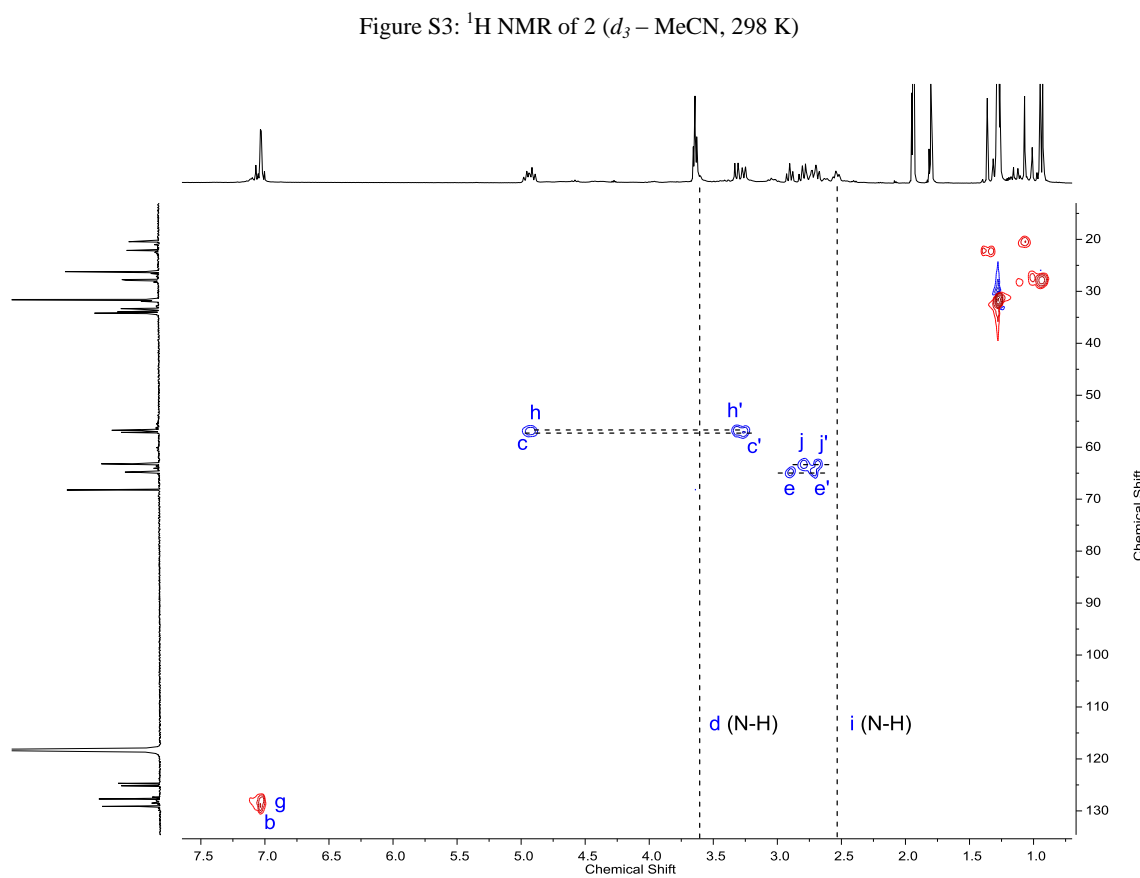
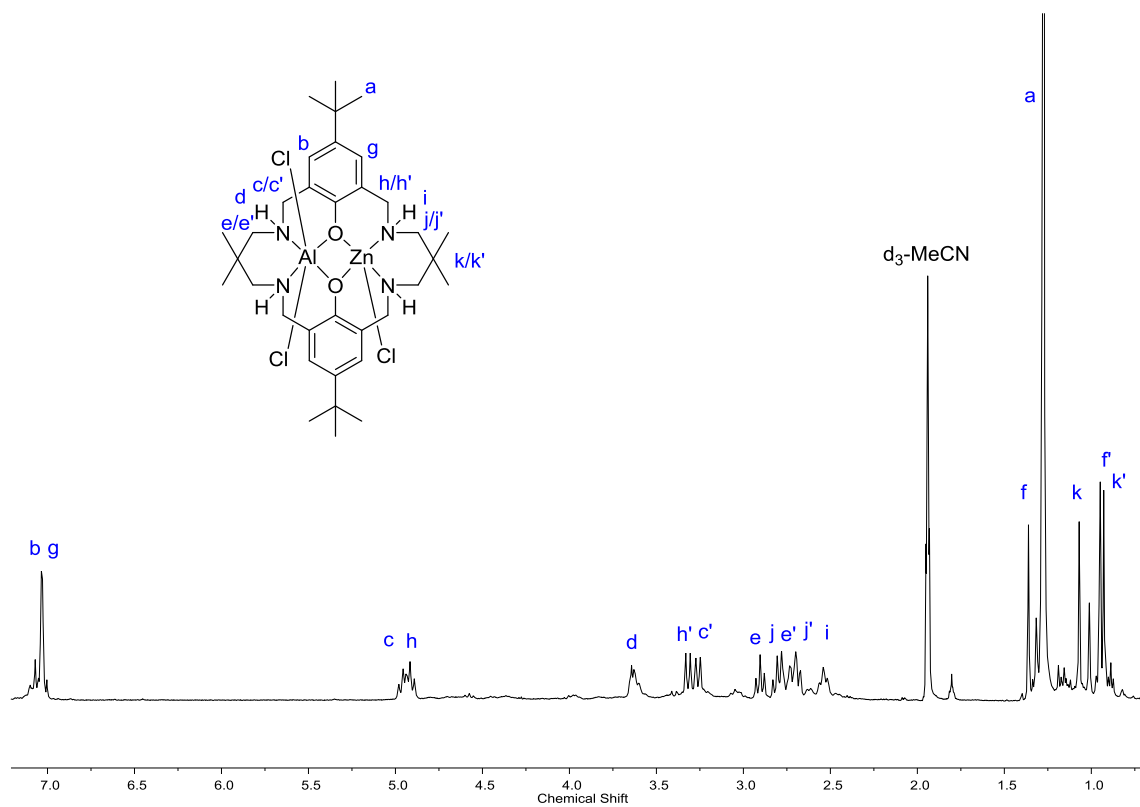


Figure S2:  $^{13}\text{C}$  NMR of **1** ( $d_2$ -TCE, 403 K)



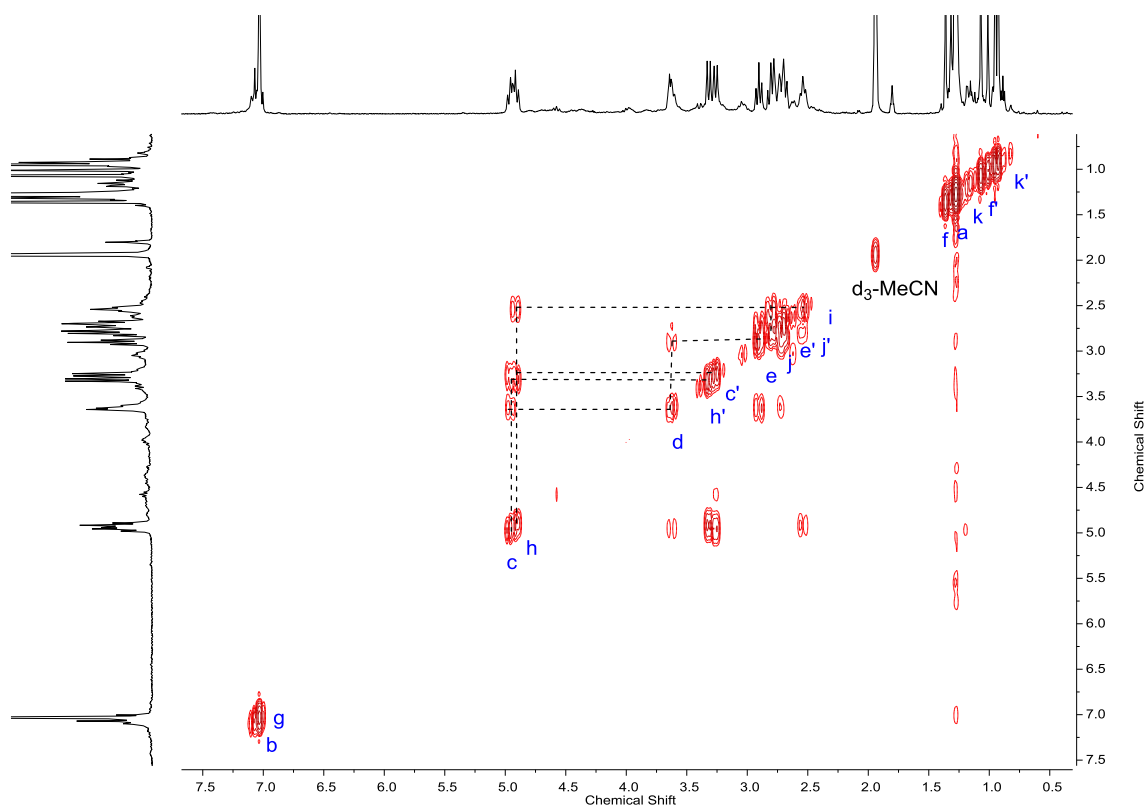


Figure S5: 2D COSY NMR of **2** ( $d_3$  – THF, 298 K)

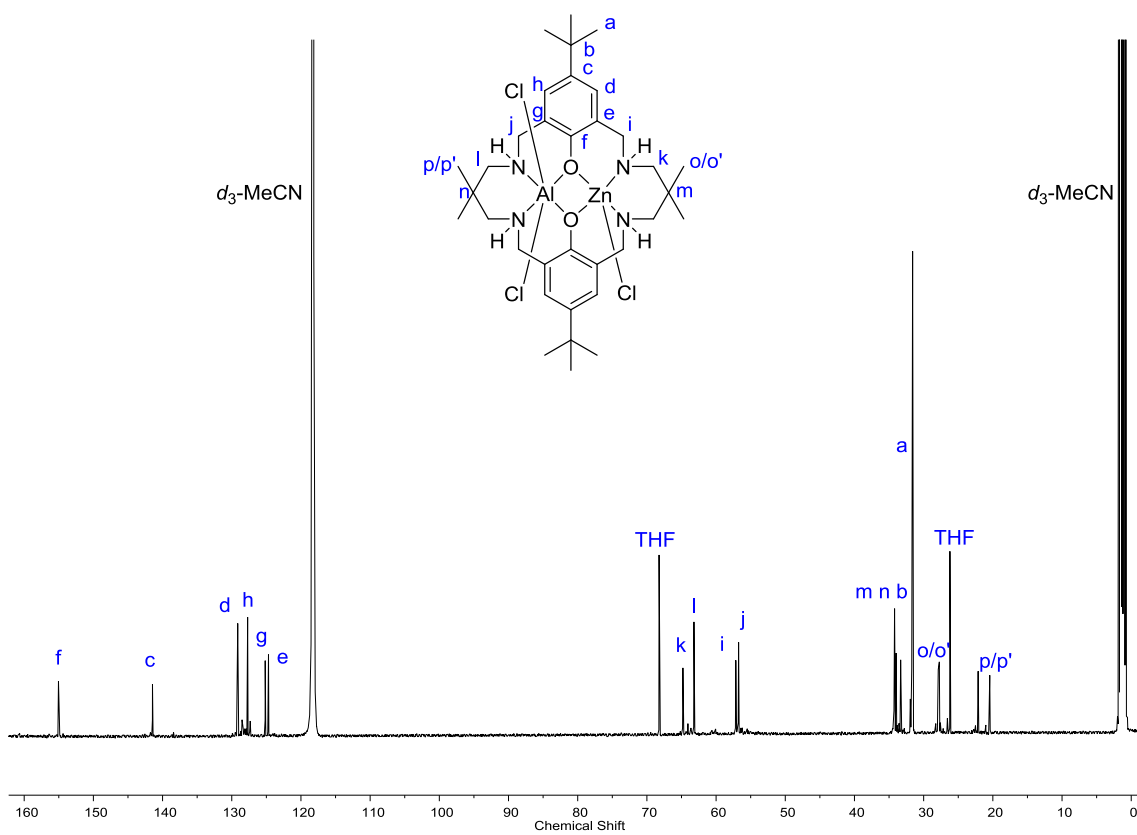


Figure S6:  $^{13}\text{C}$  NMR of **2** ( $d_3$  – MeCN, 298 K)

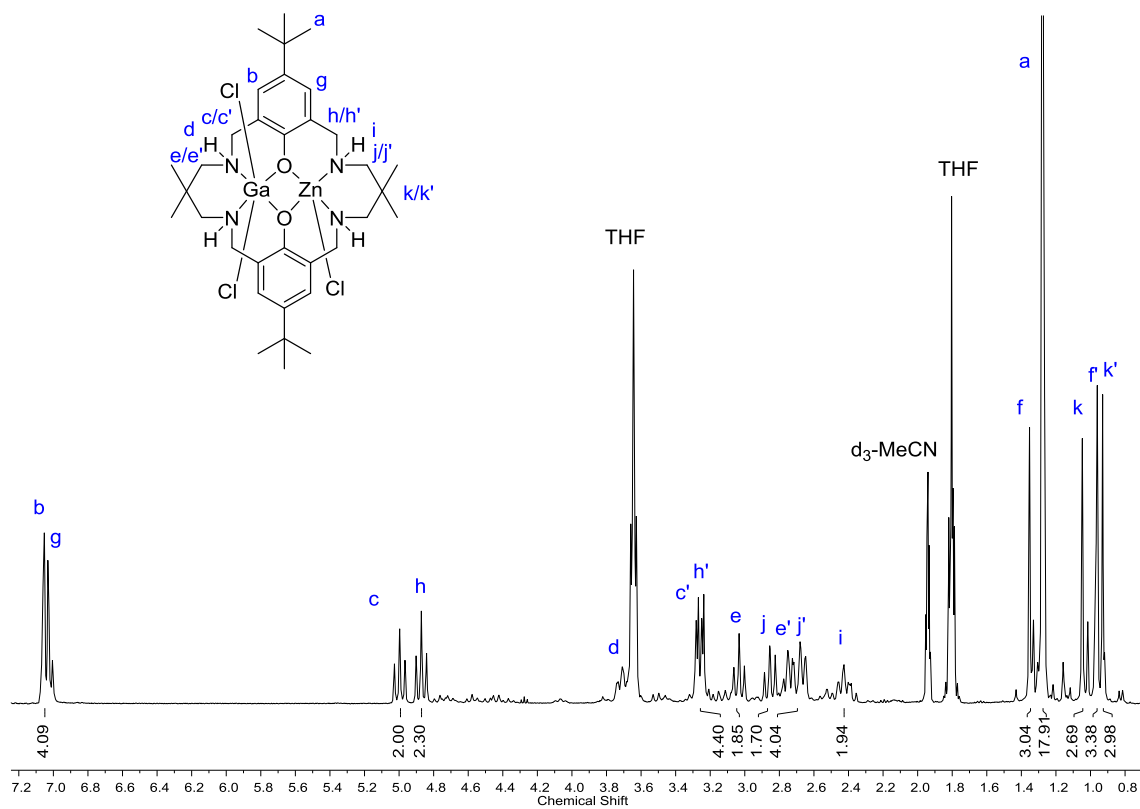


Figure S7:  $^1\text{H}$  NMR of **3** ( $d_3$  - MeCN, 298 K)

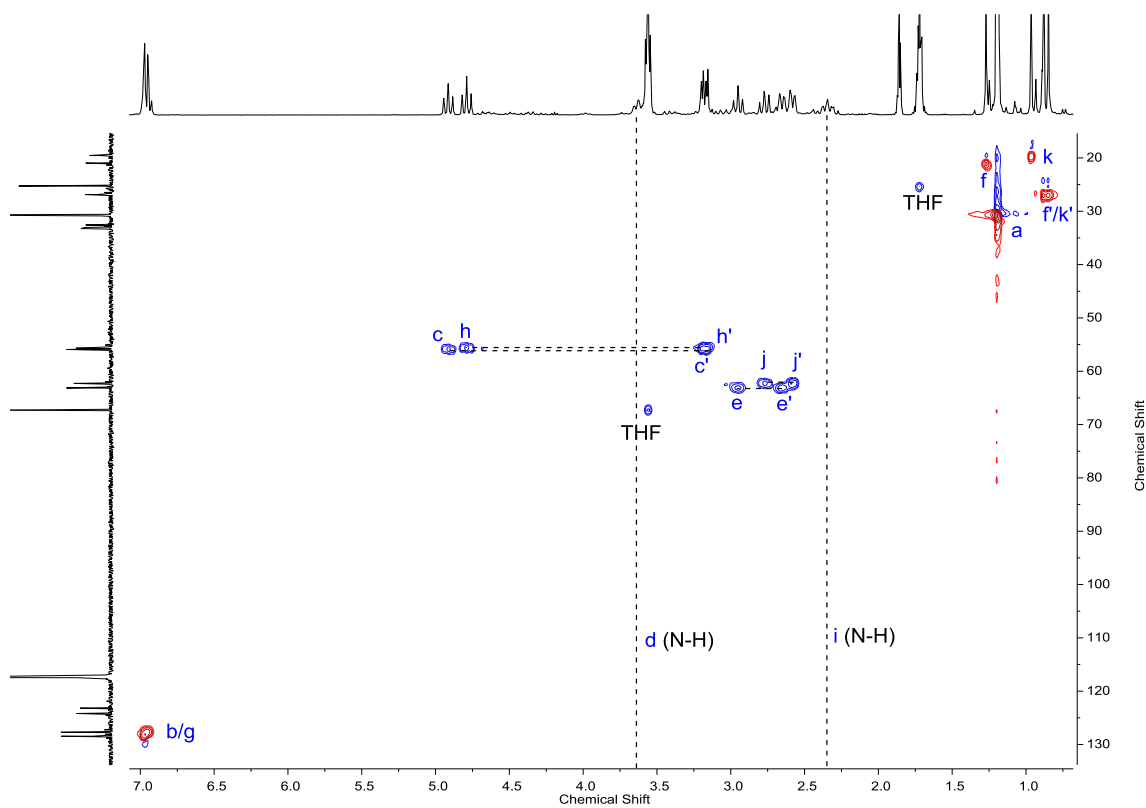


Figure S8: 2D HSQC NMR of **3** ( $d_3$  - MeCN, 298 K)

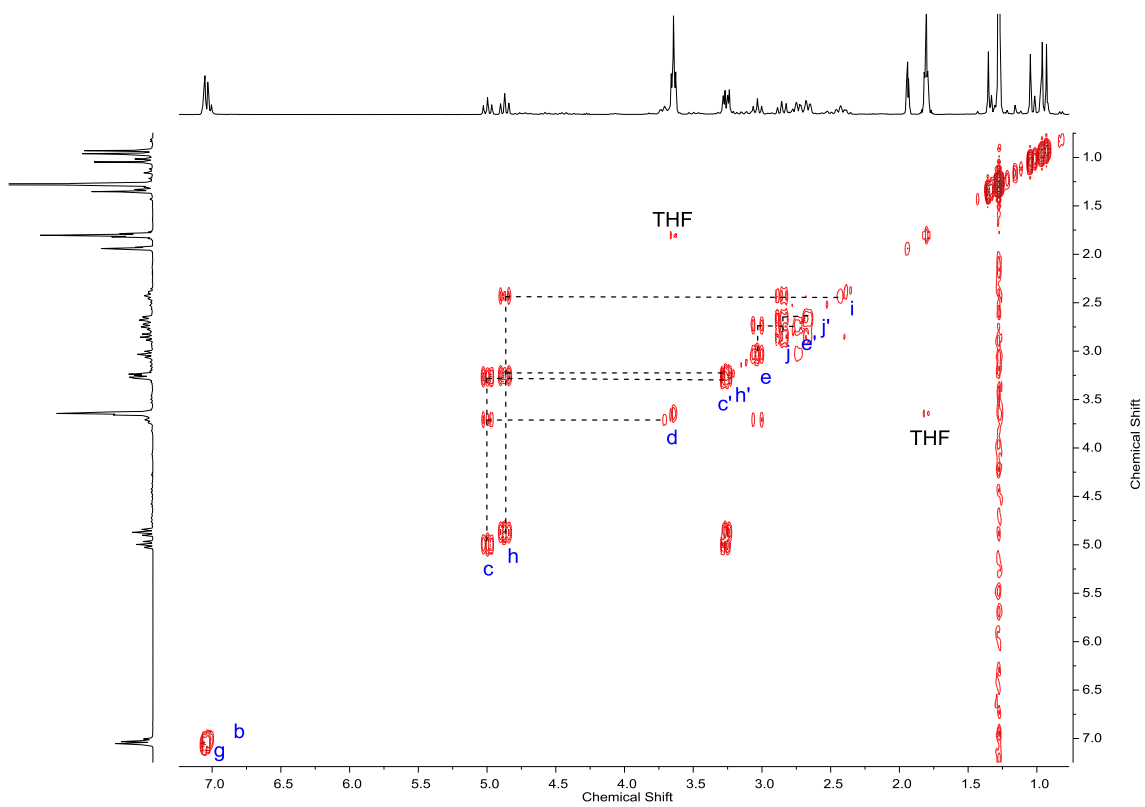


Figure S9: 2D COSY NMR of 3 ( $d_3$  - MeCN, 298 K)

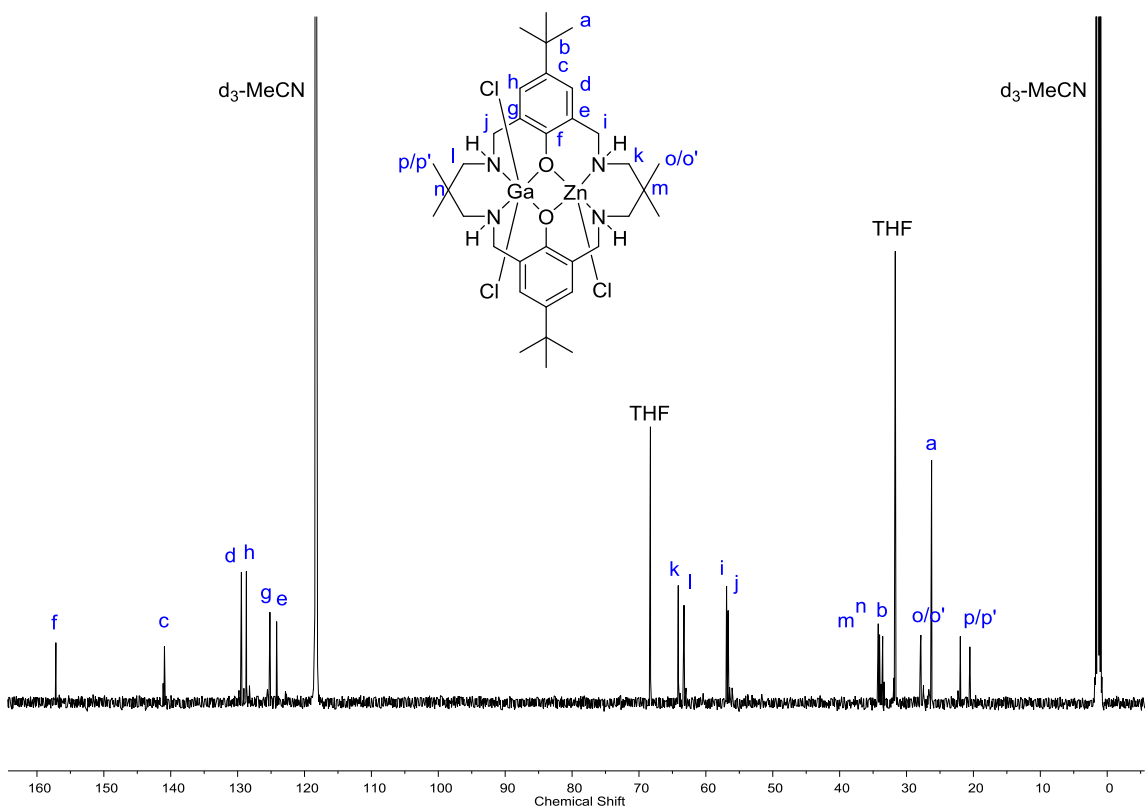


Figure S10:  $^{13}\text{C}$  NMR of 3 ( $d_3$  - MeCN, 298 K)

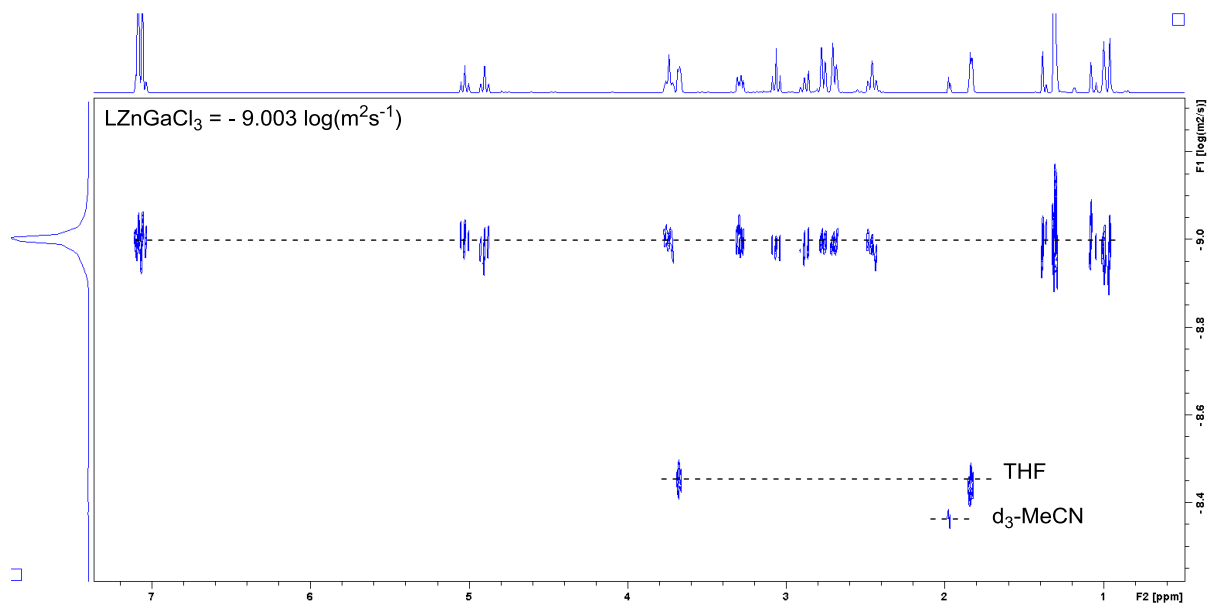


Figure S11: 2D DOSY NMR of 3 (*d*<sub>3</sub>-MeCN, 298 K)

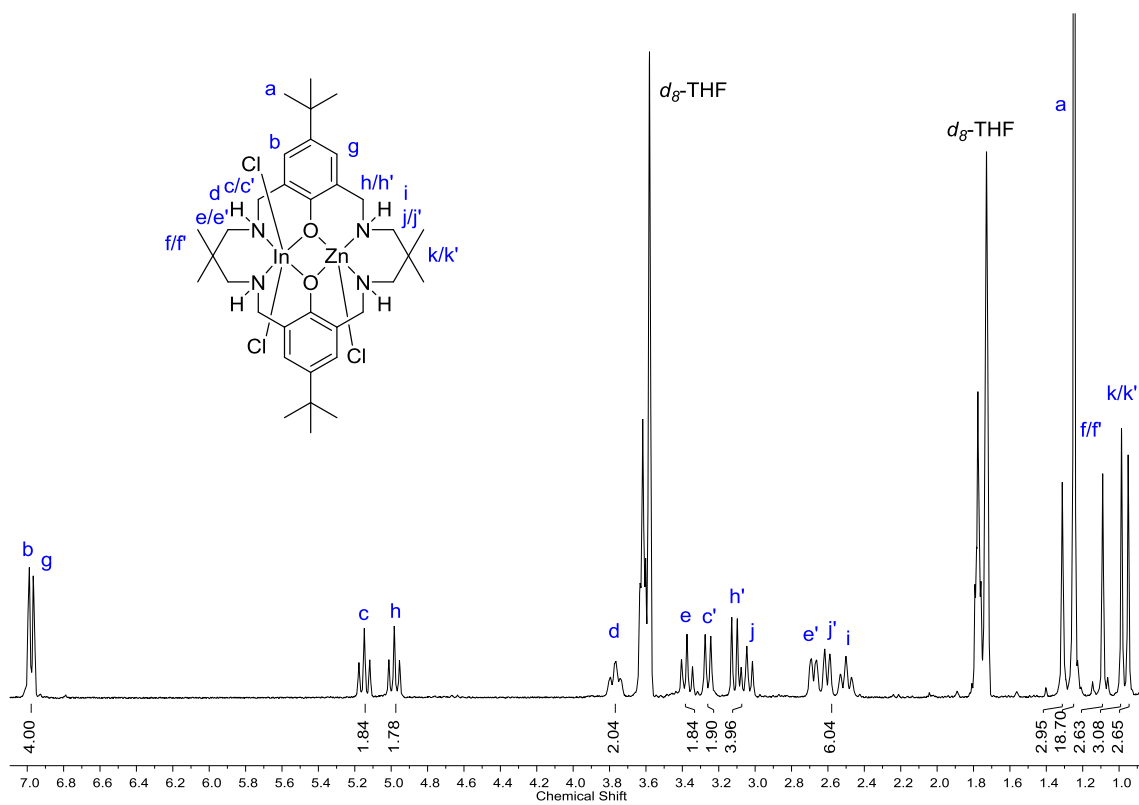


Figure S12: <sup>1</sup>H NMR of 4 (*d*<sub>8</sub>-THF, 298 K)



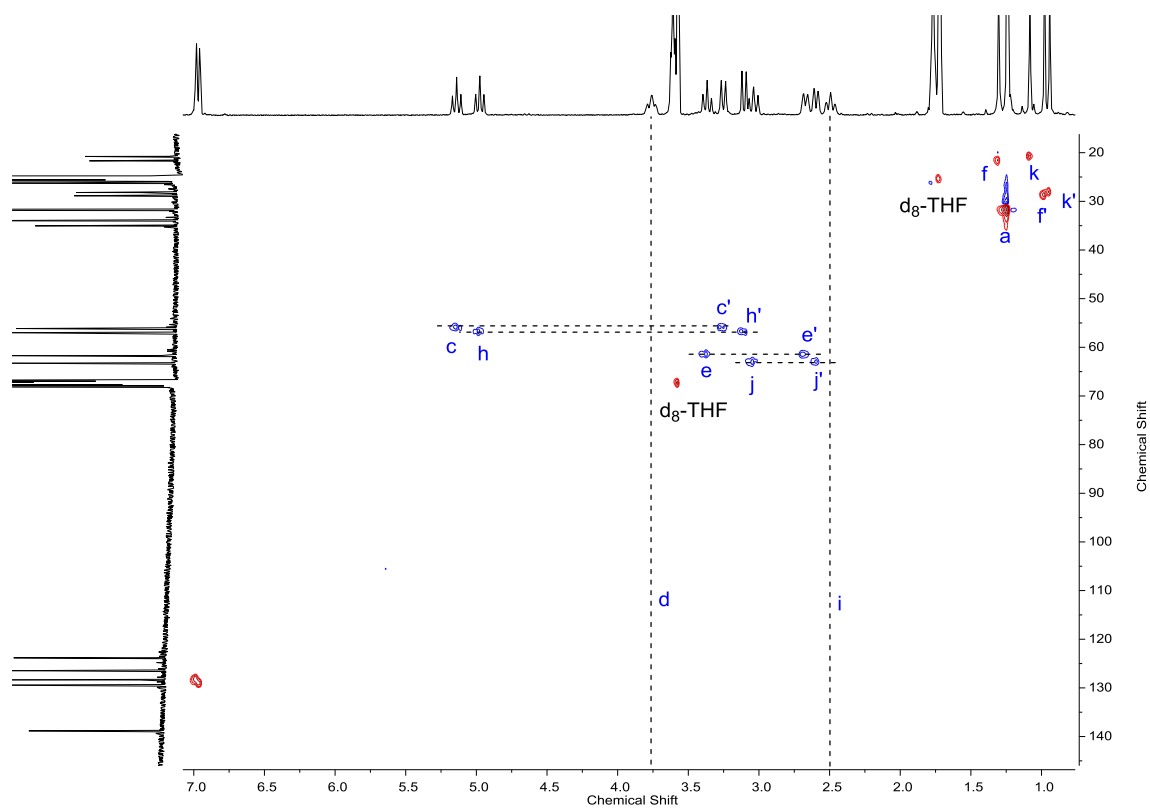


Figure S13: 2D HSQC NMR of 4 ( $d_8$ -THF, 298 K)

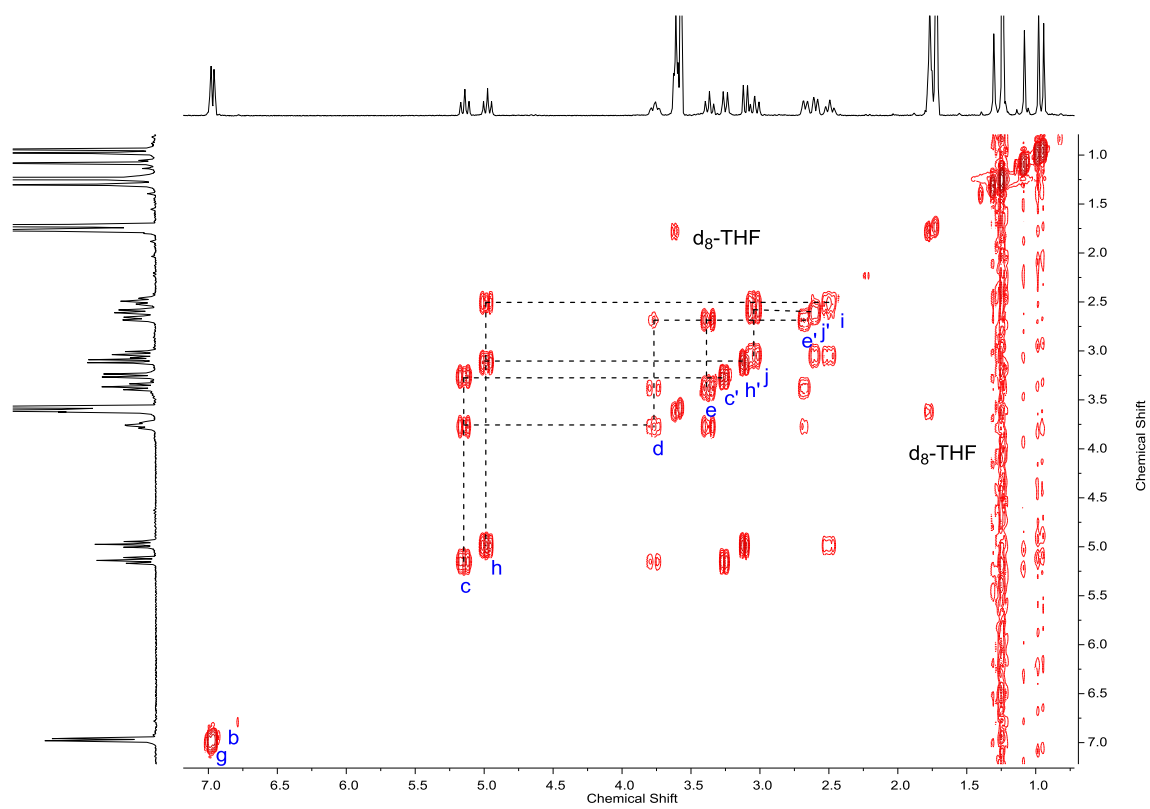


Figure S14: 2D COSY NMR of 4 ( $d_8$ -THF, 298 K)

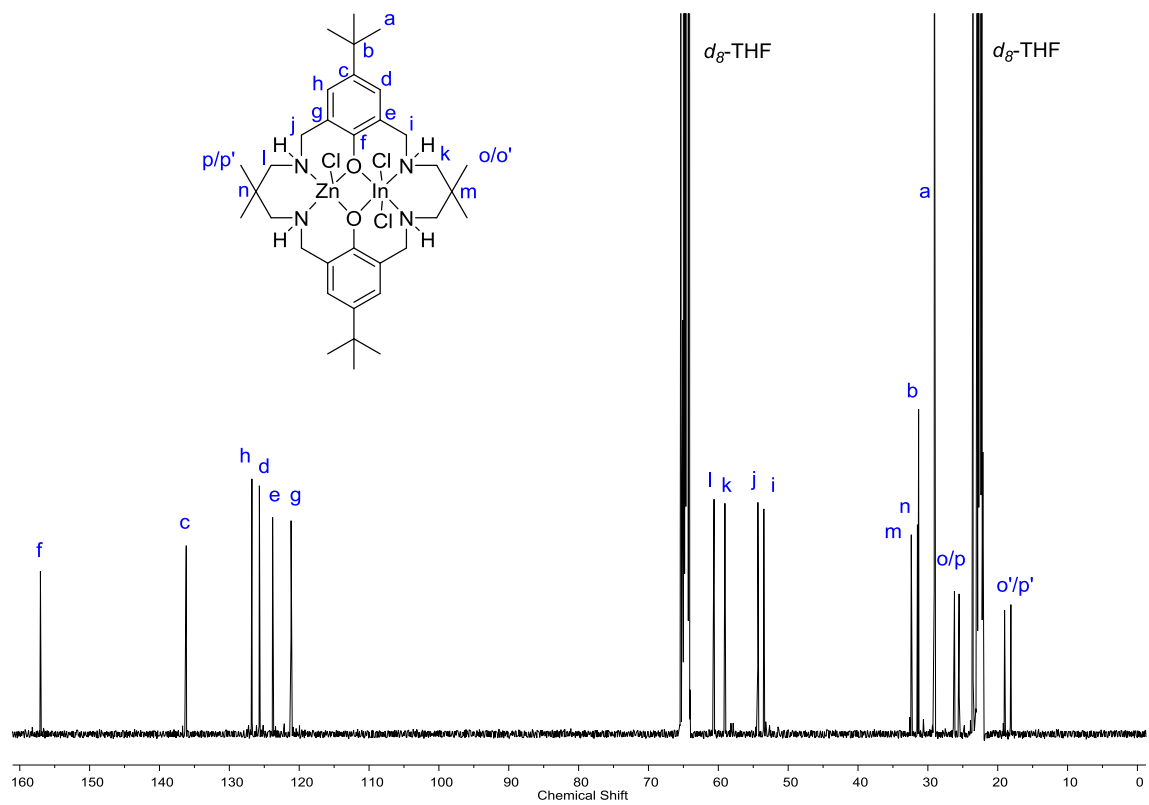


Figure S15:  $^{13}\text{C}$  NMR of 4 ( $d_8$ -THF, 298 K)

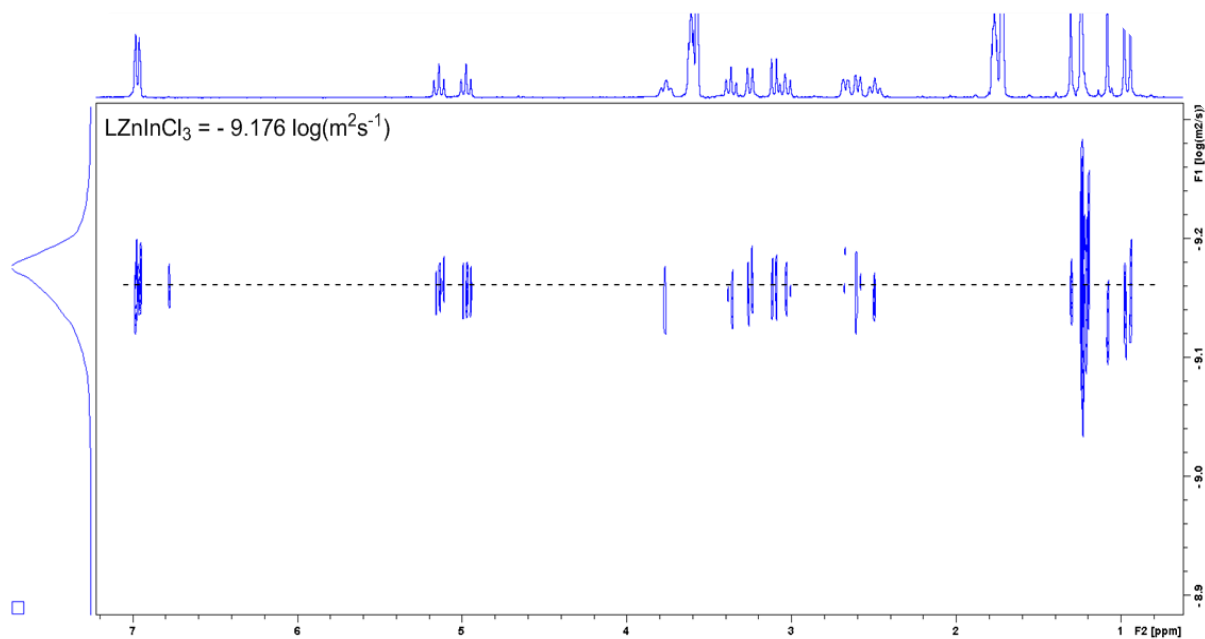


Figure S16: 2D DOSY NMR of 4 ( $d_8$ -THF, 298 K)

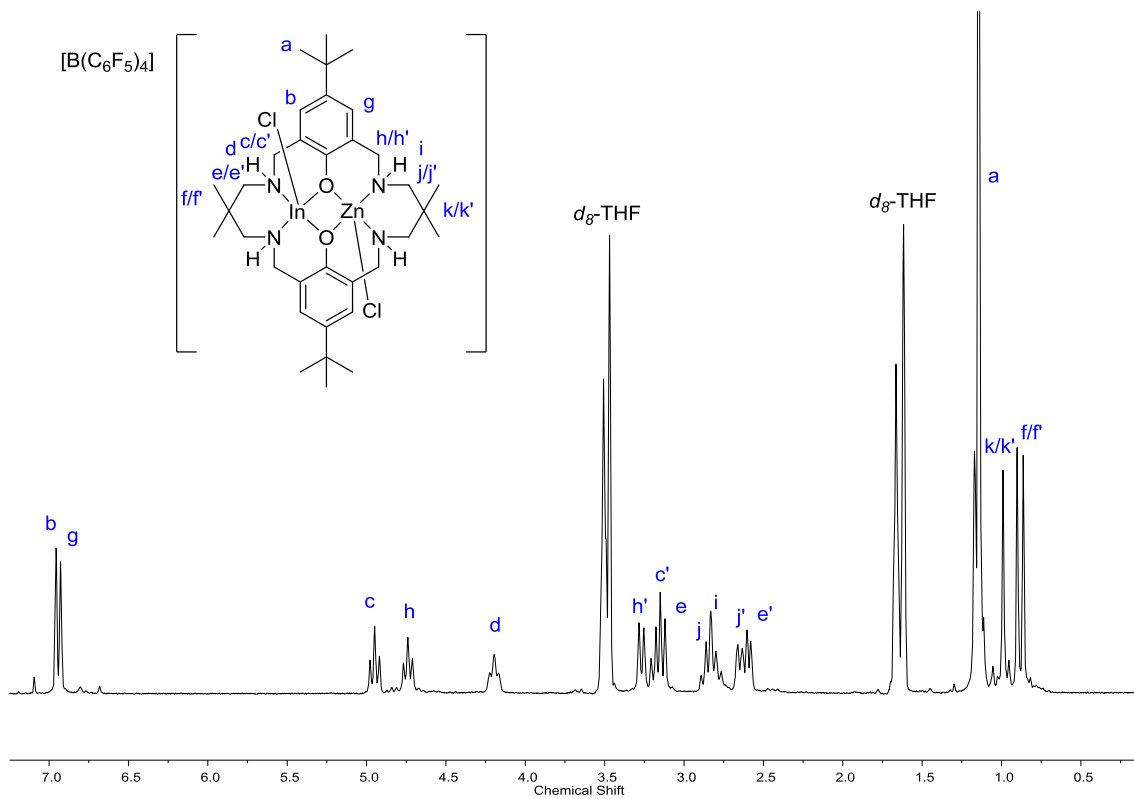


Figure S17:  $^1\text{H}$  NMR spectrum of complex **5** ( $d_8$ -THF, 298 K)

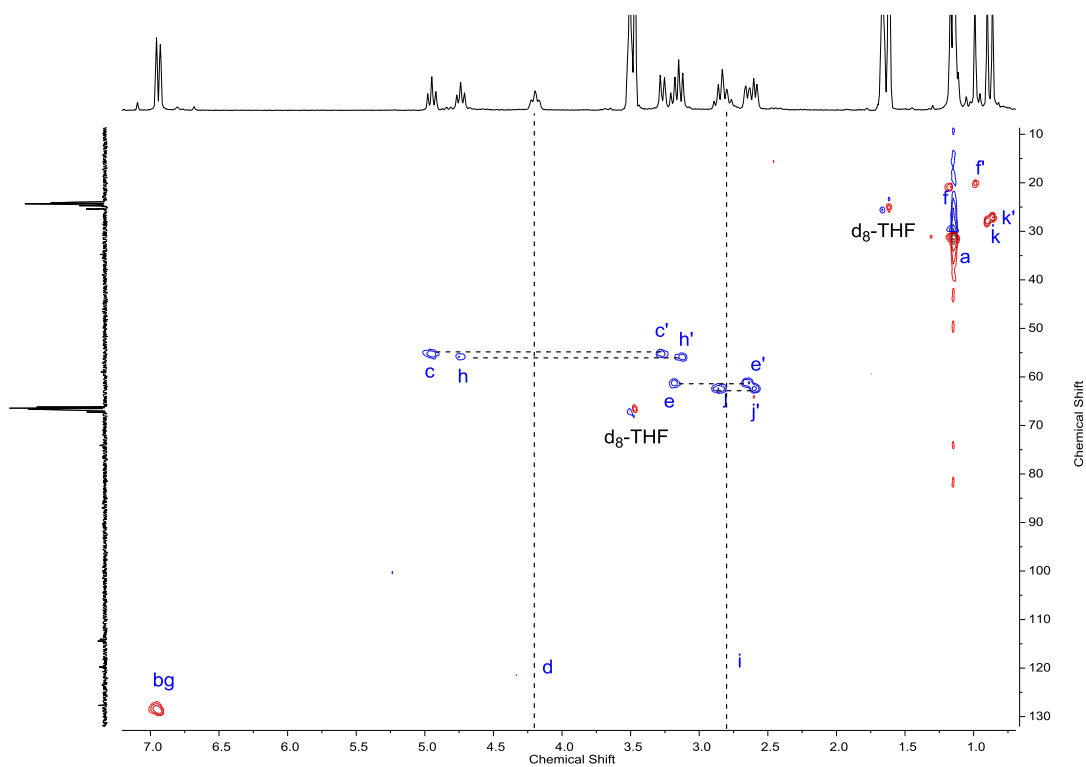


Figure S18: HSQC NMR of complex **5** ( $d_8$ -THF, 298 K)

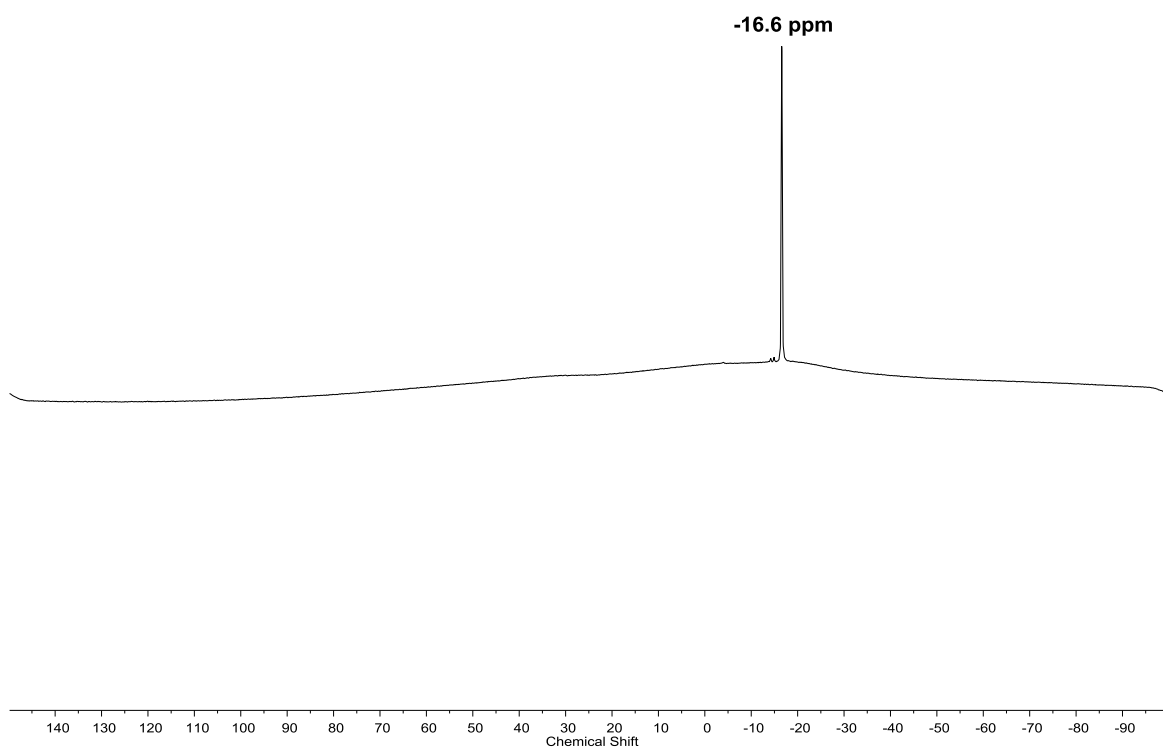


Figure S19:  $^{11}\text{B}$  NMR of complex **5** ( $d_8$ -THF, 298 K)

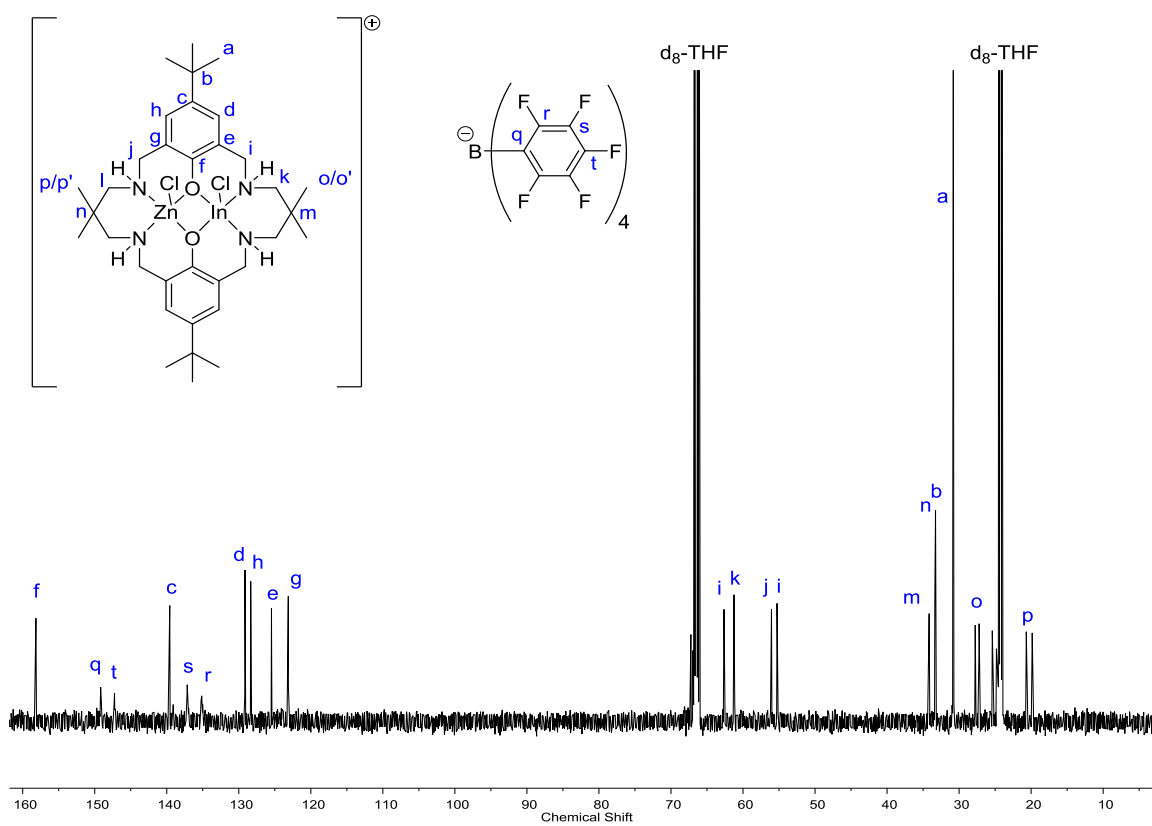


Figure S20:  $^{13}\text{C}$  NMR of complex **5** ( $d_8$ -THF, 298 K)

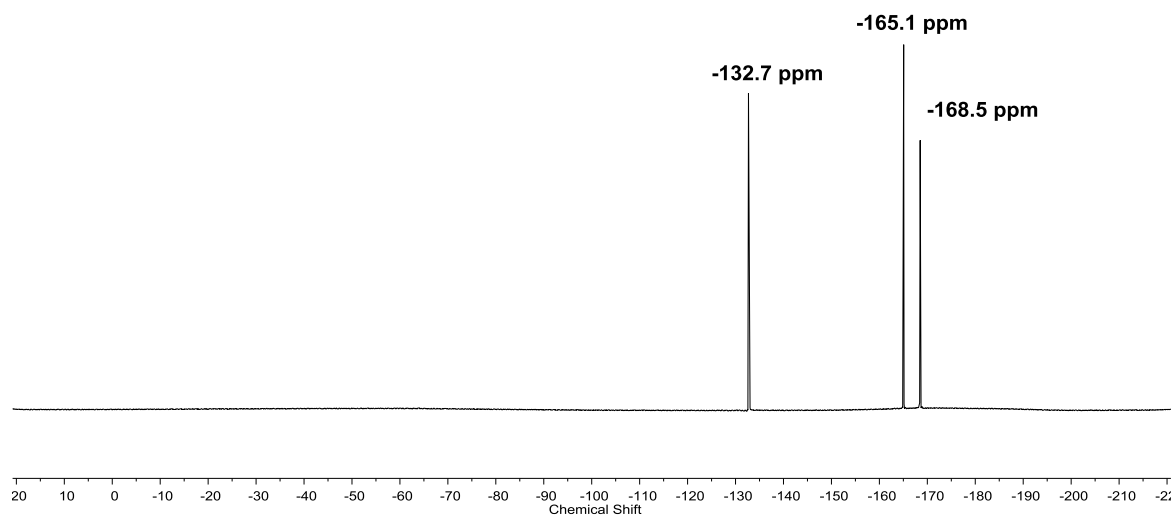


Figure S21:  $^{19}\text{F}$  NMR of complex **5** ( $d_8$ -THF, 298 K)

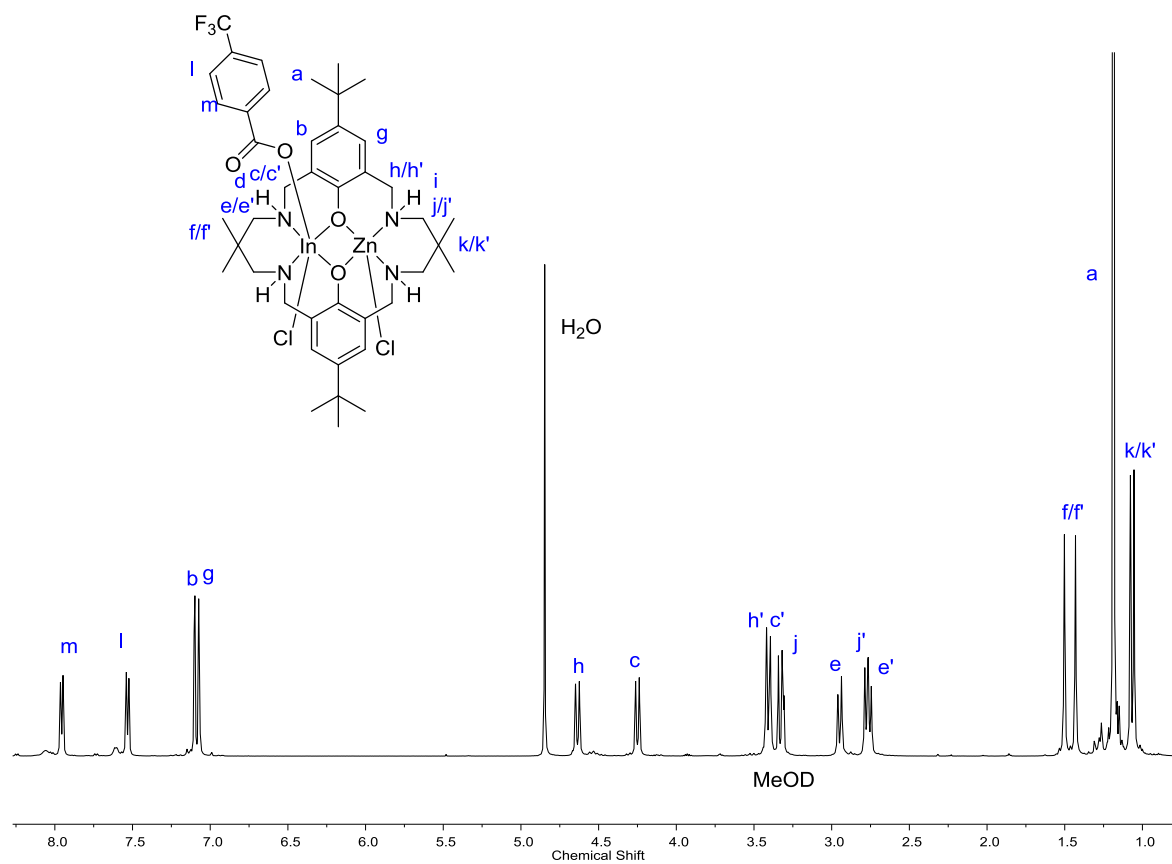


Figure S22:  $^1\text{H}$  NMR spectrum of complex **6** ( $d_4$ -MeOD, 298 K)

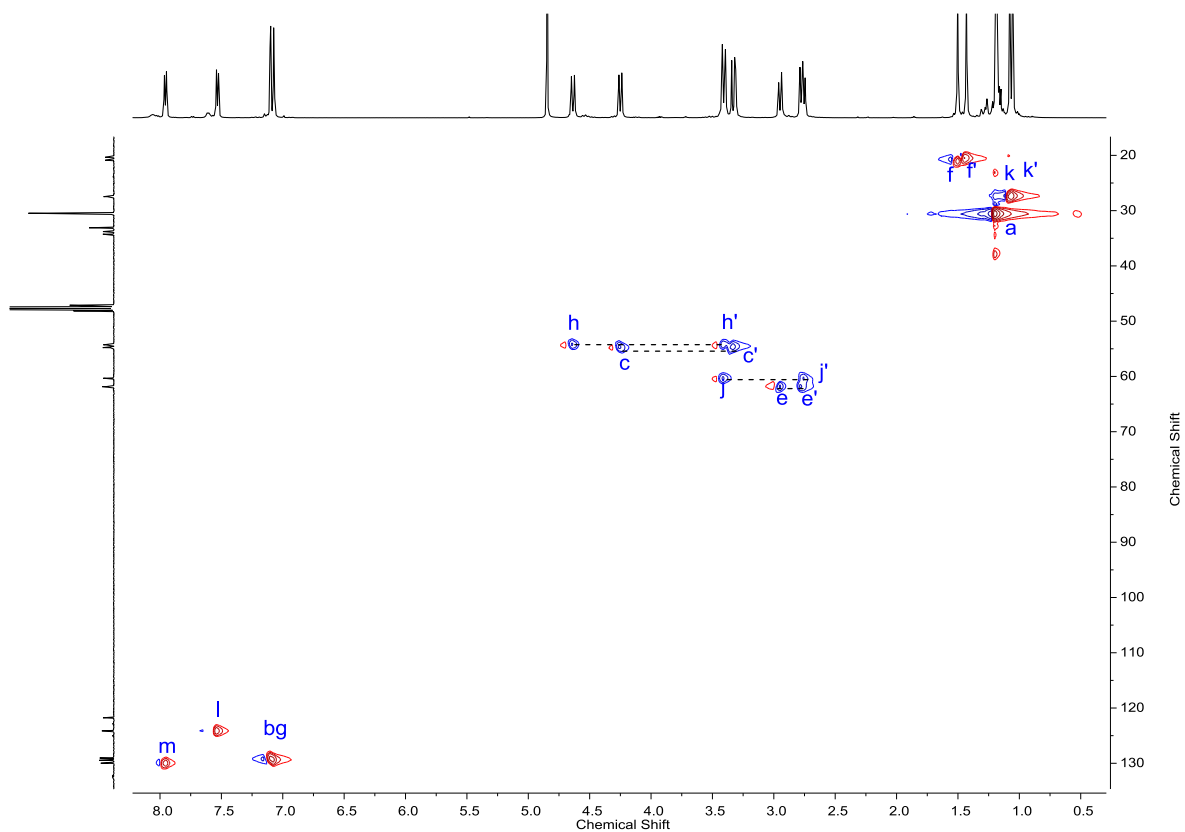


Figure S23: HSQC NMR of complex **6** ( $d_4$ -MeOD, 298 K)

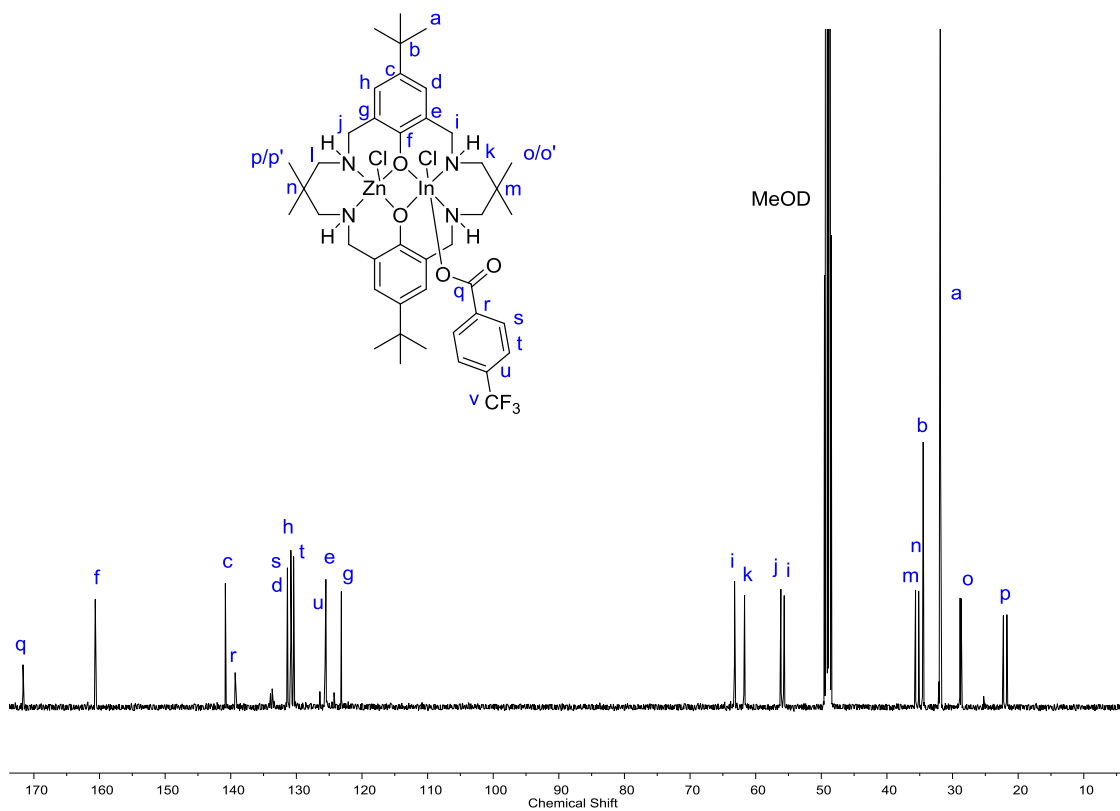


Figure S24:  $^{13}\text{C}$  NMR of complex **6** ( $d_4$ -MeOD, 298 K)

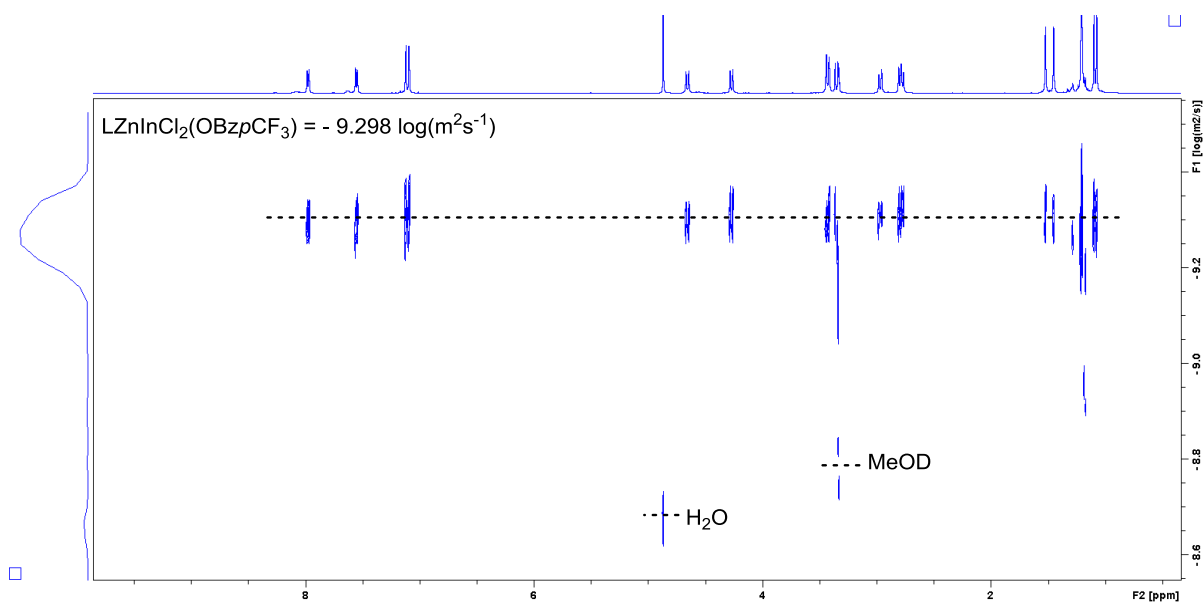


Figure S25: 2D DOSY NMR of complex **6** (d<sub>4</sub>-MeOD, 298 K)

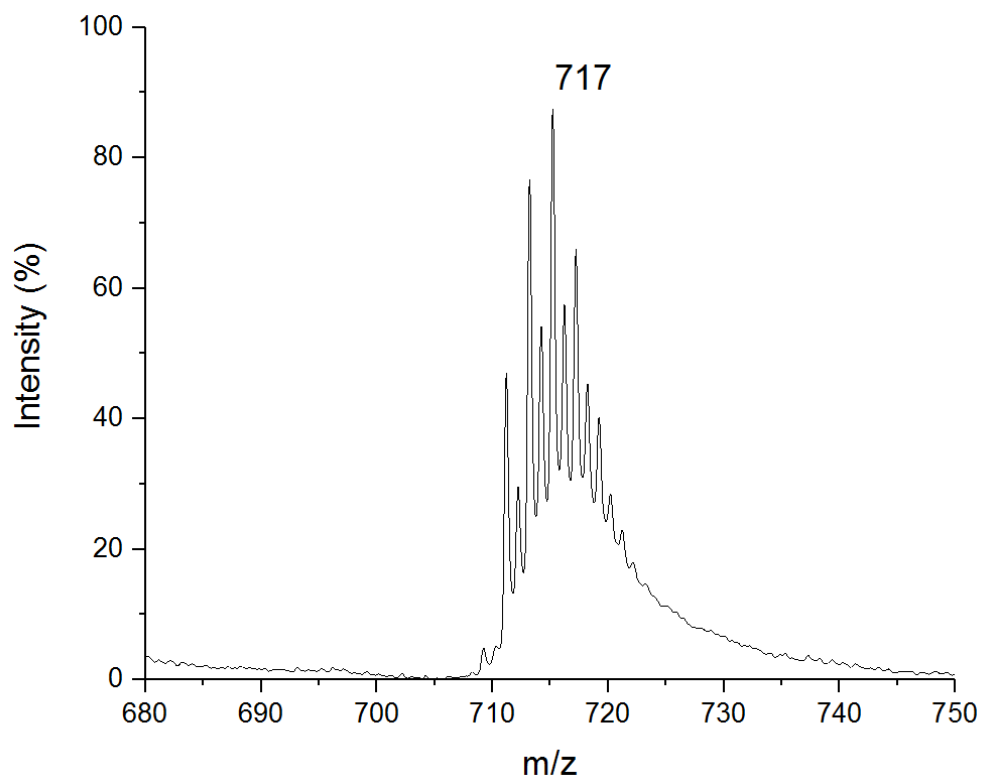


Figure S26: MALDI – ToF mass spectrum of **1**

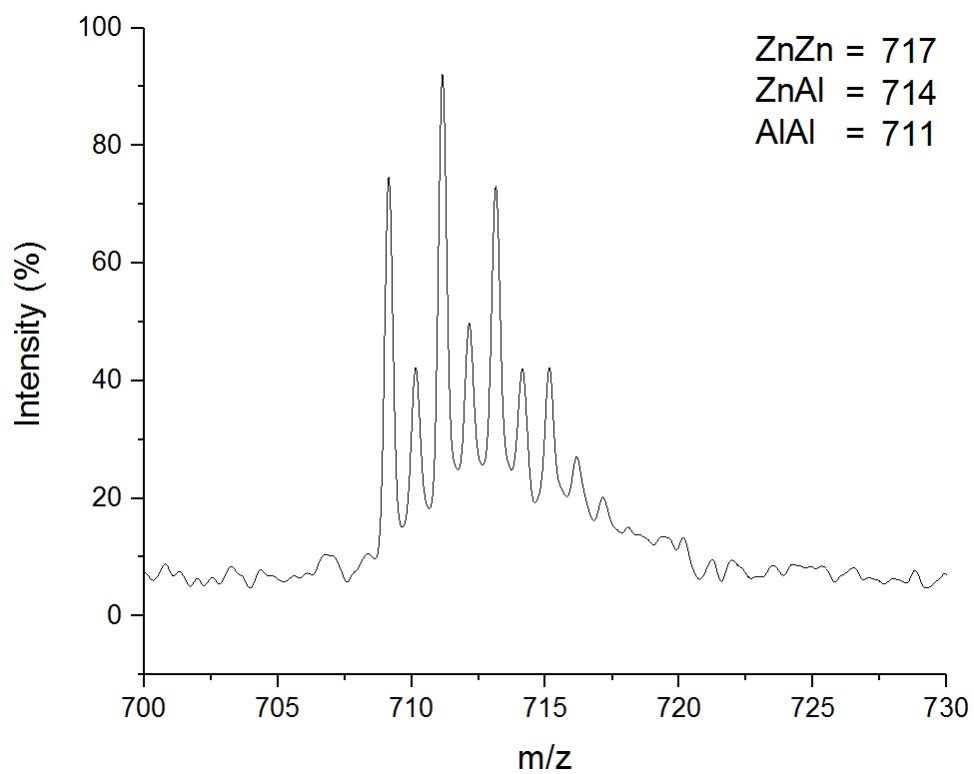


Figure S27: MALDI – ToF mass spectrum of 2

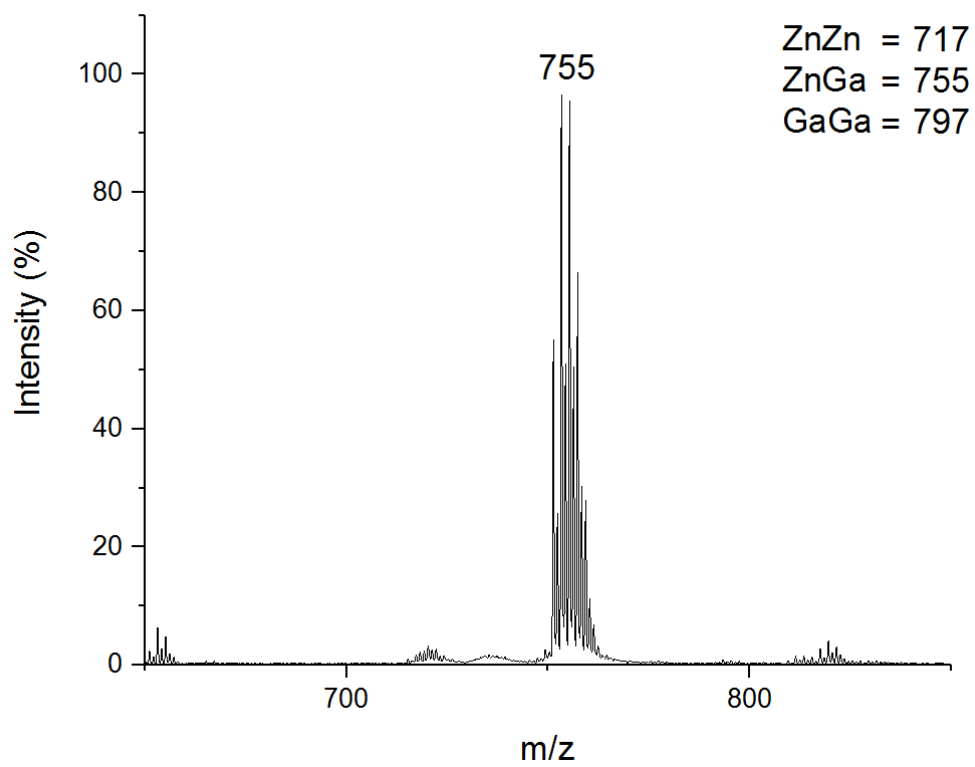


Figure S28: MALDI – ToF mass spectrum of 3



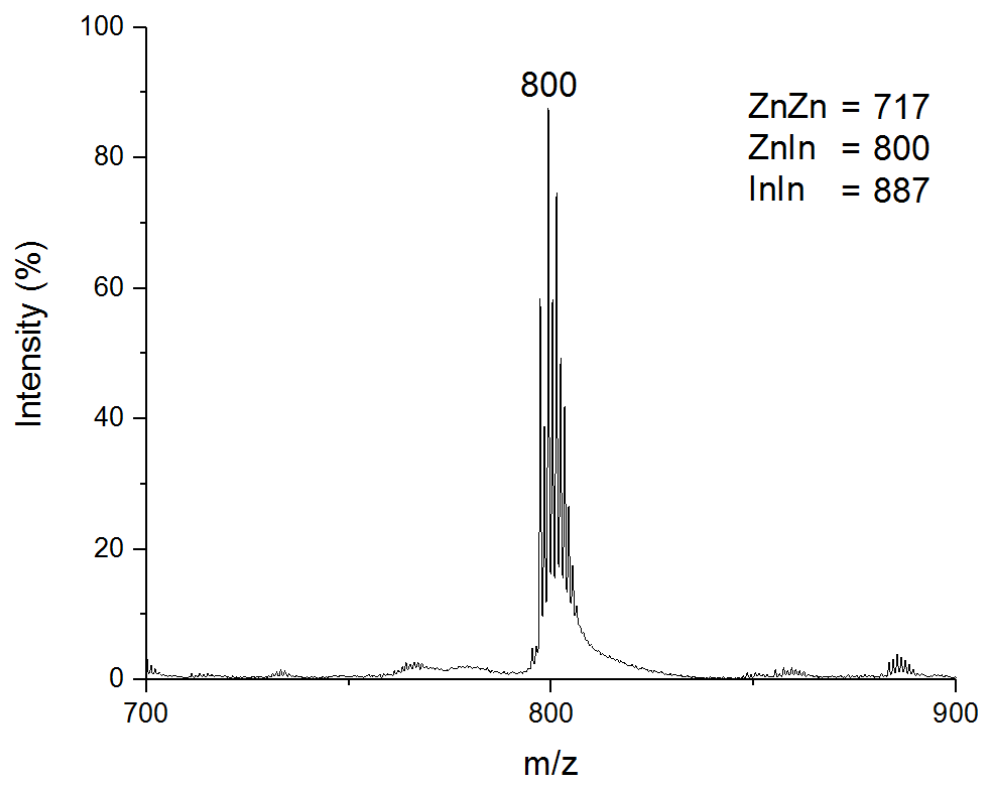


Figure S29: MALDI – ToF mass spectrum of 4

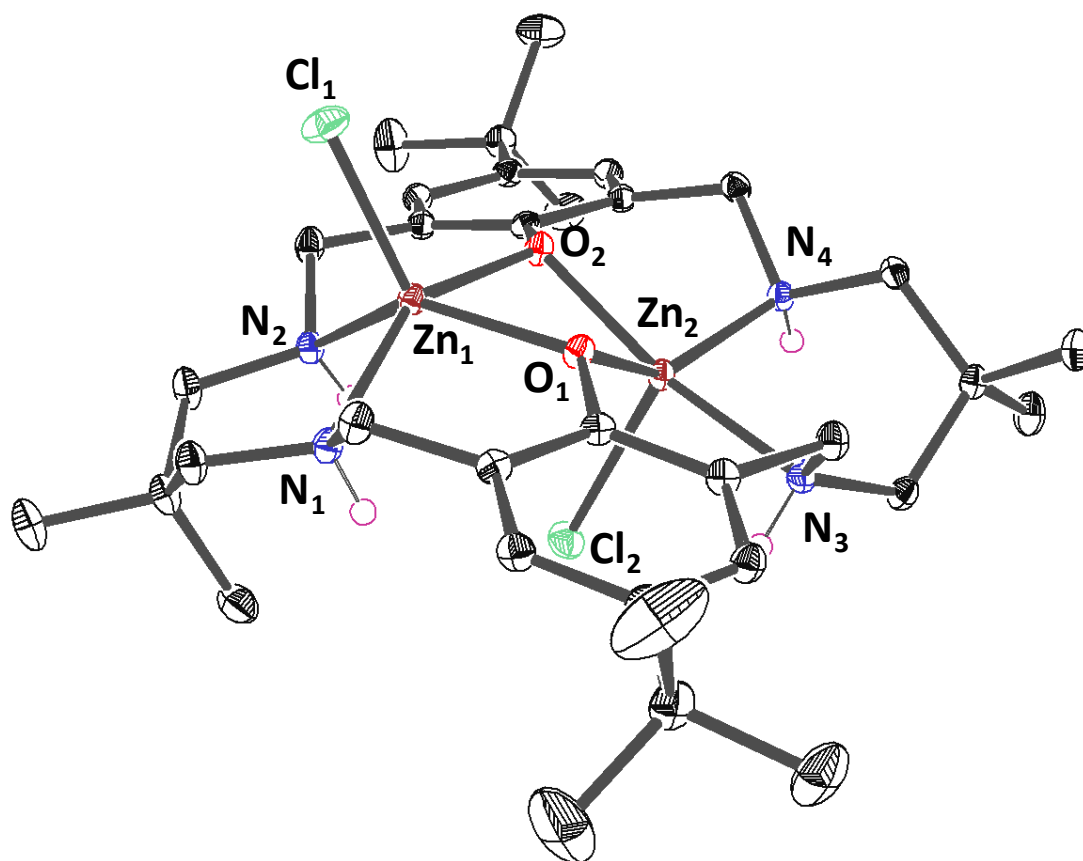


Figure S30: ORTEP representation of the molecular structure of **1** with disorder and hydrogen atoms (excluding NH) omitted for clarity with thermal ellipsoids represented at 40 % probability.

Table S1: Selected bond lengths (Å) and angles (°) for complex **1**.

Bond	Bond Length (Å)	Bond	Bond Angle (°)
N (1) – Zn (1)	2.10(6)	N (1) – Zn (1) – O (2)	162.3(1)
N (2) – Zn (1)	2.10(8)	N (2) – Zn (1) – O (1)	141.2(9)
O (1) – Zn (1)	2.07(7)	Cl (1) – Zn (1) – O (1)	100.8(9)
O (2) – Zn (1)	2.03(5)	N (3) – Zn (2) – O (2)	148.1(7)
Cl (1) – Zn (1)	2.31(1)	N (4) – Zn (2) – O (1)	139.4(5)
N (3) – Zn (2)	2.11(3)	Cl (2) – Zn (2) – O (1)	112.9(4)
N (4) – Zn (2)	2.14(3)	<b>Metal – Metal</b>	<b>Distance (Å)</b>
O (1) – Zn (2)	2.11(2)	Zn (1) – Zn (2)	3.04(0)
O (2) – Zn (2)	2.04(9)		
Cl (2) – Zn (2)	2.25(9)		

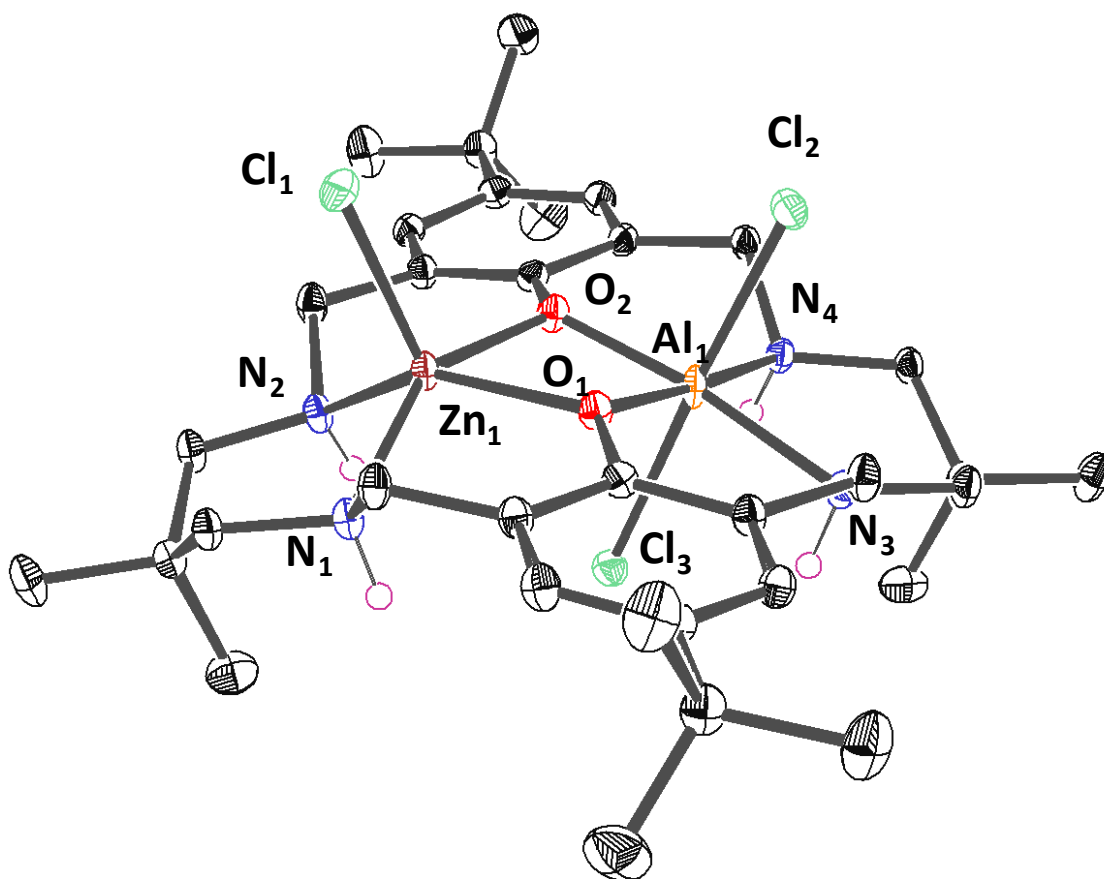


Figure S31: ORTEP representation of the molecular structure of **2** with disorder and hydrogen atoms (excluding NH) omitted for clarity with thermal ellipsoids represented at 40 % probability.

Table S2: Selected bond lengths (Å) and angles (°) for complex **2**.

Bond	Bond Length (Å)	Bond	Bond Angle (°)
N (1) – Zn (1)	2.08(9)	N (1) – Zn (1) – O (2)	148.6(0)
N (2) – Zn (1)	2.09(0)	N (2) – Zn (1) – O (1)	144.3(1)
O (1) – Zn (1)	2.08(6)	Cl (1) – Zn (1) – O (1)	109.1(9)
O (2) – Zn (1)	2.04(6)	N (3) – Al (1) – O (2)	172.6(1)
Cl (1) – Zn (1)	2.28(9)	N (4) – Al (1) – O (1)	175.2(6)
N (3) – Al (1)	2.09(3)	Cl (2) – Al (1) – Cl (3)	176.8(9)
N (4) – Al (1)	2.06(0)	<b>Metal – Metal</b>	<b>Distance (Å)</b>
O (1) – Al (1)	1.92(4)	Zn (1) – Al (1)	3.02(3)
O (2) – Al (1)	1.89(1)		
Cl (2) – Al (1)	2.33(3)		
Cl (3) – Al (1)	2.41(2)		

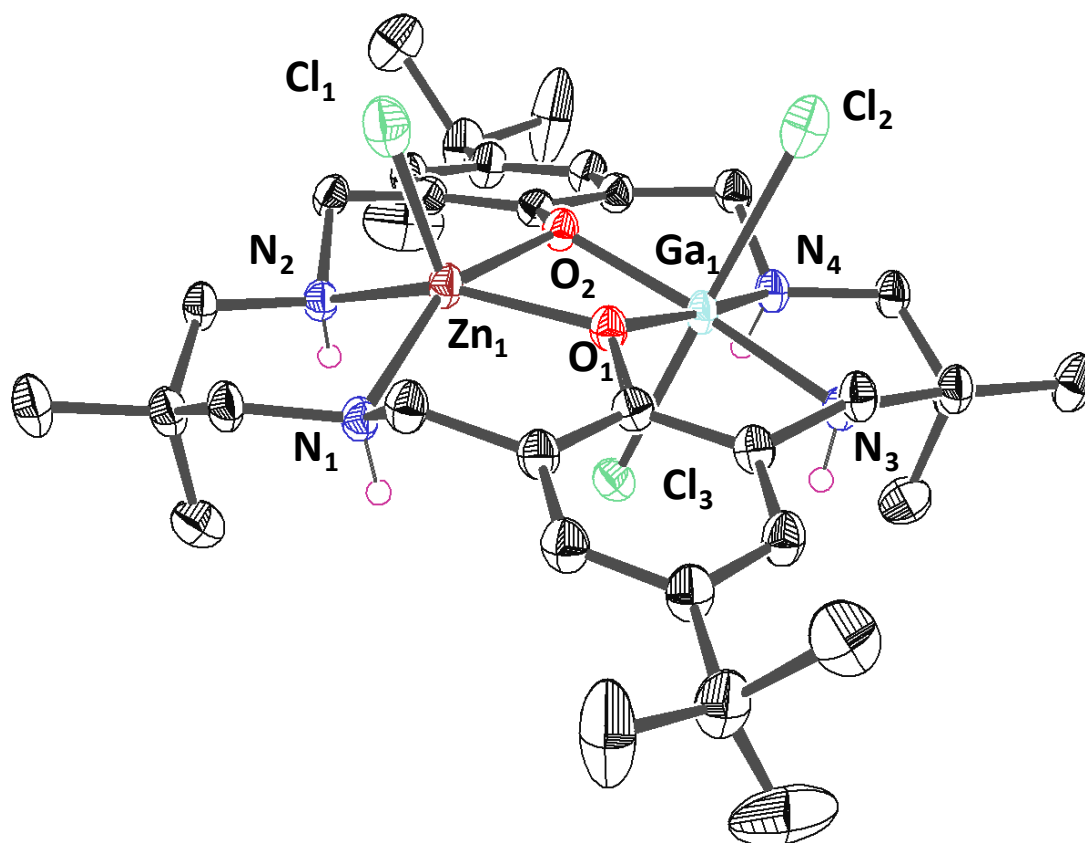


Figure S32: ORTEP representation of the molecular structure of **3** with disorder and hydrogen atoms (excluding NH) omitted for clarity with thermal ellipsoids represented at 40 % probability.

Table S3: Selected bond lengths (Å) and angles (°) for complex **3**.

Bond	Bond Length (Å)	Bond	Bond Angle (°)
N (1) – Zn (1)	2.13(3)	N (1) – Zn (1) – O (2)	153.7(7)
N (2) – Zn (1)	2.10(3)	N (2) – Zn (1) – O (1)	152.6(0)
O (1) – Zn (1)	2.11(7)	Cl (1) – Zn (1) – O (1)	106.3(5)
O (2) – Zn (1)	2.06(9)	N (3) – Ga (1) – O (2)	174.0(0)
Cl (1) – Zn (1)	2.11(1)	N (4) – Ga (1) – O (1)	172.7(4)
N (3) – Ga (1)	2.06(2)	Cl (2) – Ga (1) – Cl (3)	178.7(3)
N (4) – Ga (1)	2.09(9)	<b>Metal – Metal</b>	<b>Distance (Å)</b>
O (1) – Ga (1)	2.01(9)	Zn (1) – Ga (1)	3.12(3)
O (2) – Ga (1)	2.02(6)		
Cl (2) – Ga (1)	2.54(5)		
Cl (3) – Ga (1)	2.37(2)		

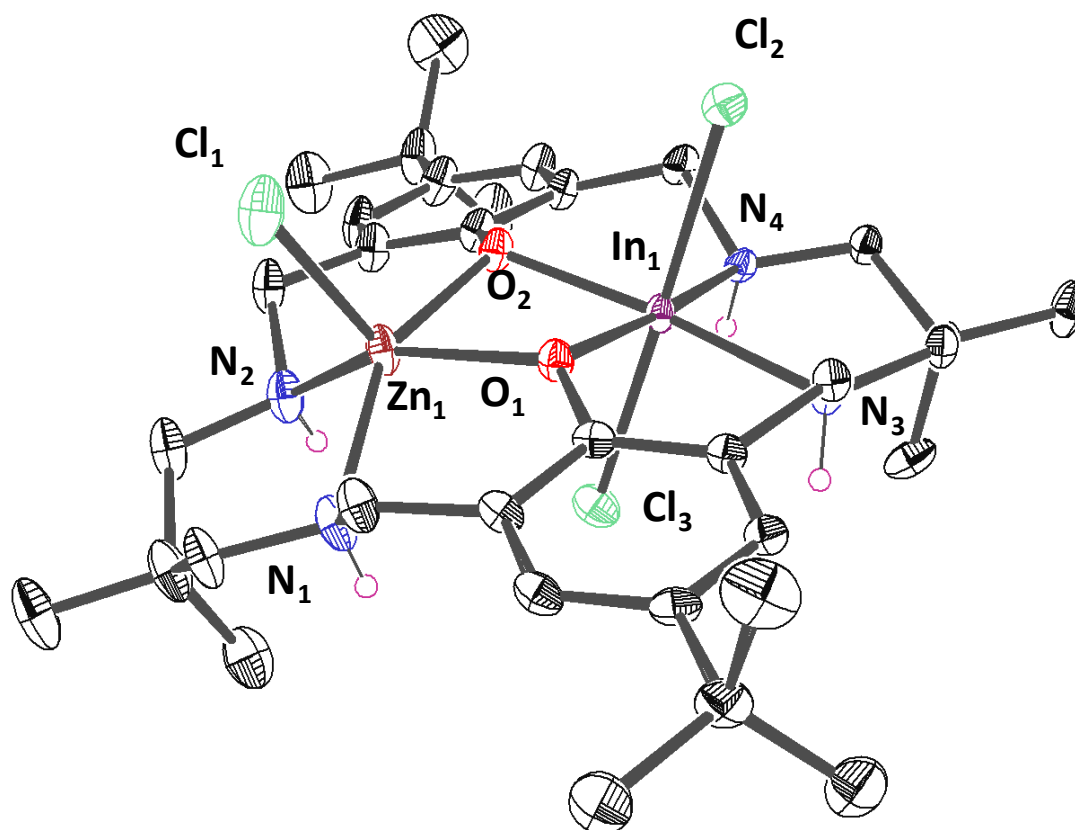


Figure S33: ORTEP representation of the molecular structure of **4** with disorder and hydrogen atoms (excluding NH) omitted for clarity with thermal ellipsoids represented at 40 % probability.

Table S4: Selected bond lengths (Å) and angles (°) for complex **4**.

Bond	Bond Length (Å)	Bond	Bond Angle (°)
N (1) – Zn (1)	2.23(8)	N (1) – Zn (1) – O (2)	150.8(9)
N (2) – Zn (1)	2.16(5)	N (2) – Zn (1) – O (1)	151.3(8)
O (1) – Zn (1)	2.27(4)	Cl (1) – Zn (1) – O (1)	103.4(6)
O (2) – Zn (1)	2.20(3)	N (3) – In (1) – O (2)	174.3(3)
Cl (1) – Zn (1)	2.06(1)	N (4) – In (1) – O (1)	173.3(8)
N (3) – In (1)	2.11(1)	Cl (2) – In (1) – Cl (3)	175.1(8)
N (4) – In (1)	2.09(4)	<b>Metal – Metal</b>	<b>Distance (Å)</b>
O (1) – In (1)	2.08(5)	Zn (1) – In (1)	3.15(8)
O (2) – In (1)	2.03(6)		
Cl (2) – In (1)	2.80(8)		
Cl (3) – In (1)	2.54(3)		

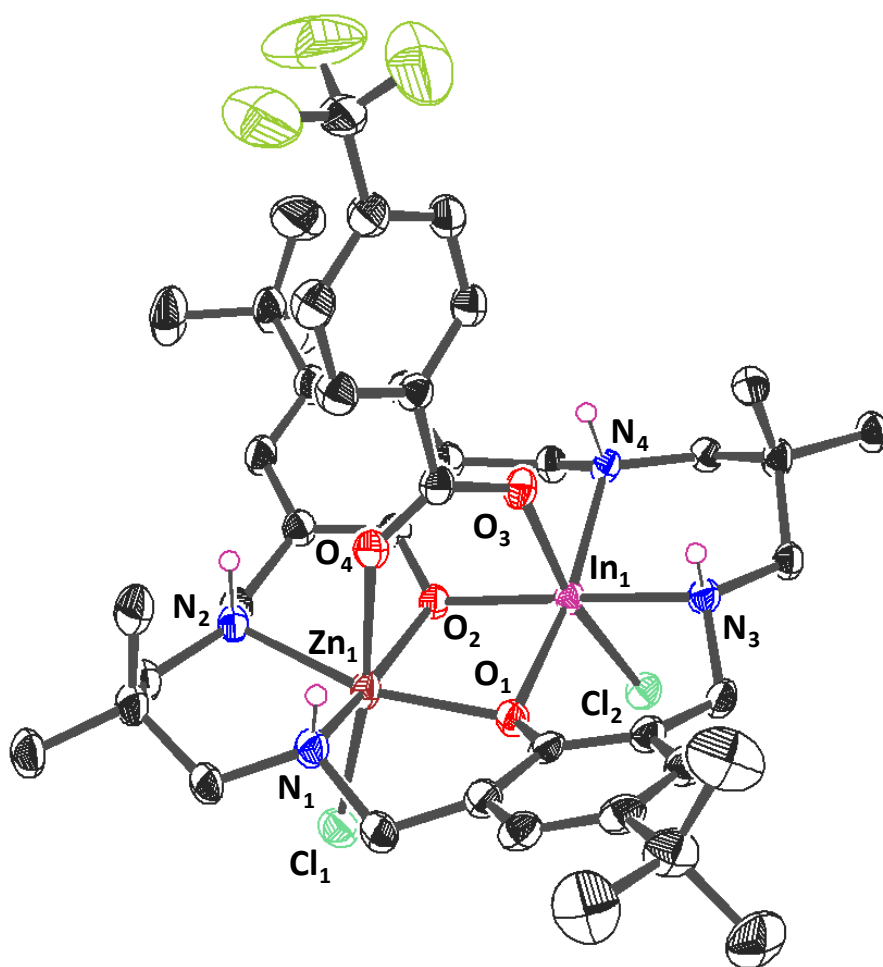
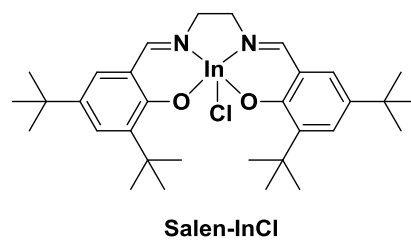
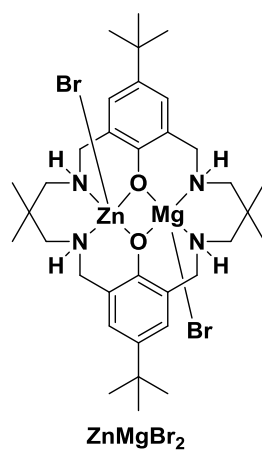
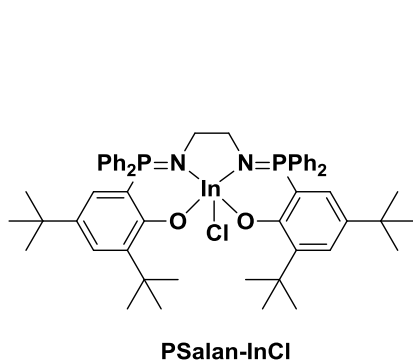


Figure S34: Connectivity data of the molecular structure of **6** with disorder and hydrogen atoms (excluding NH) omitted for clarity with thermal ellipsoids represented at 40 % probability.

### Catalyst Systems



### Catalyst-Co-Catalyst Systems

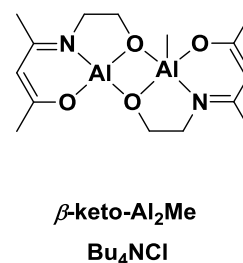
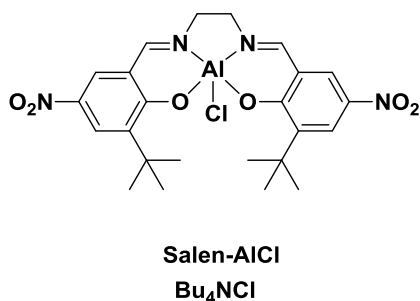
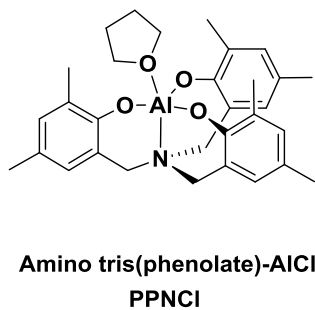


Figure S35: Molecular structures of other Group 13 active for CO<sub>2</sub>/CHO ROCOP.

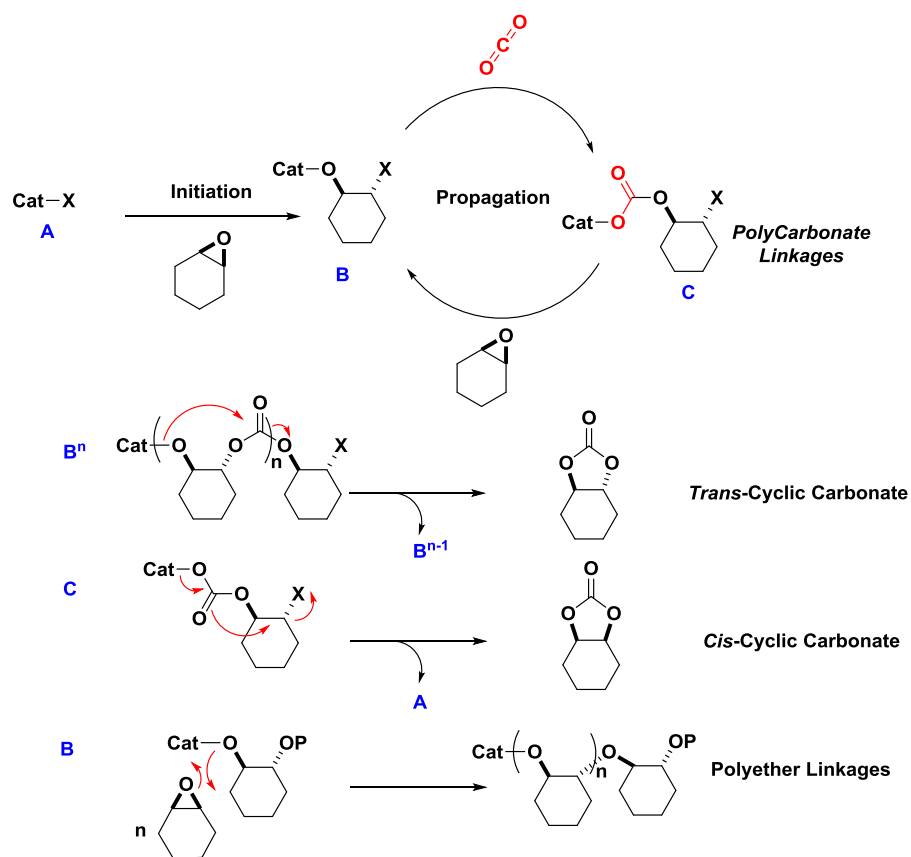


Figure S36: Illustration of the catalytic cycle to polycarbonate formation, along with side reactions resulting in cyclic carbonate and polyether linkages.

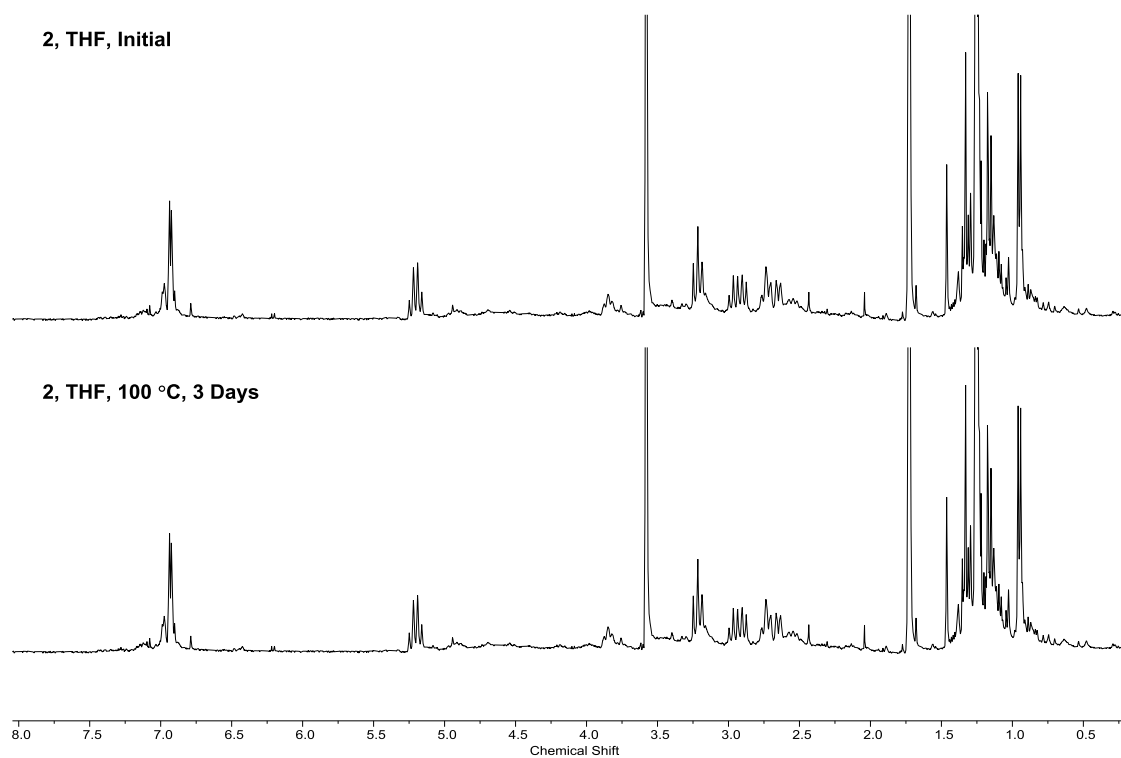


Figure S37: Complex **2** heated to 100 °C in THF for 3 days



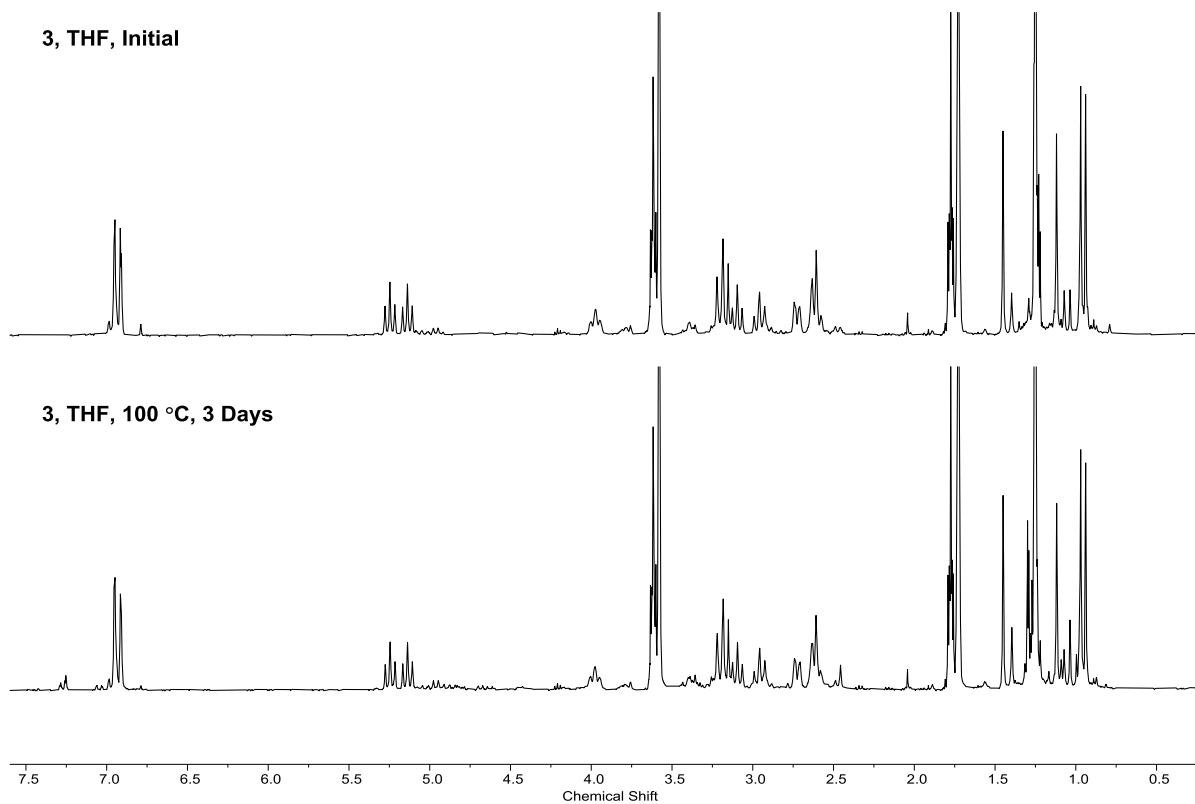


Figure S38 : Complex **3** heated to 100 °C in THF for 3 days

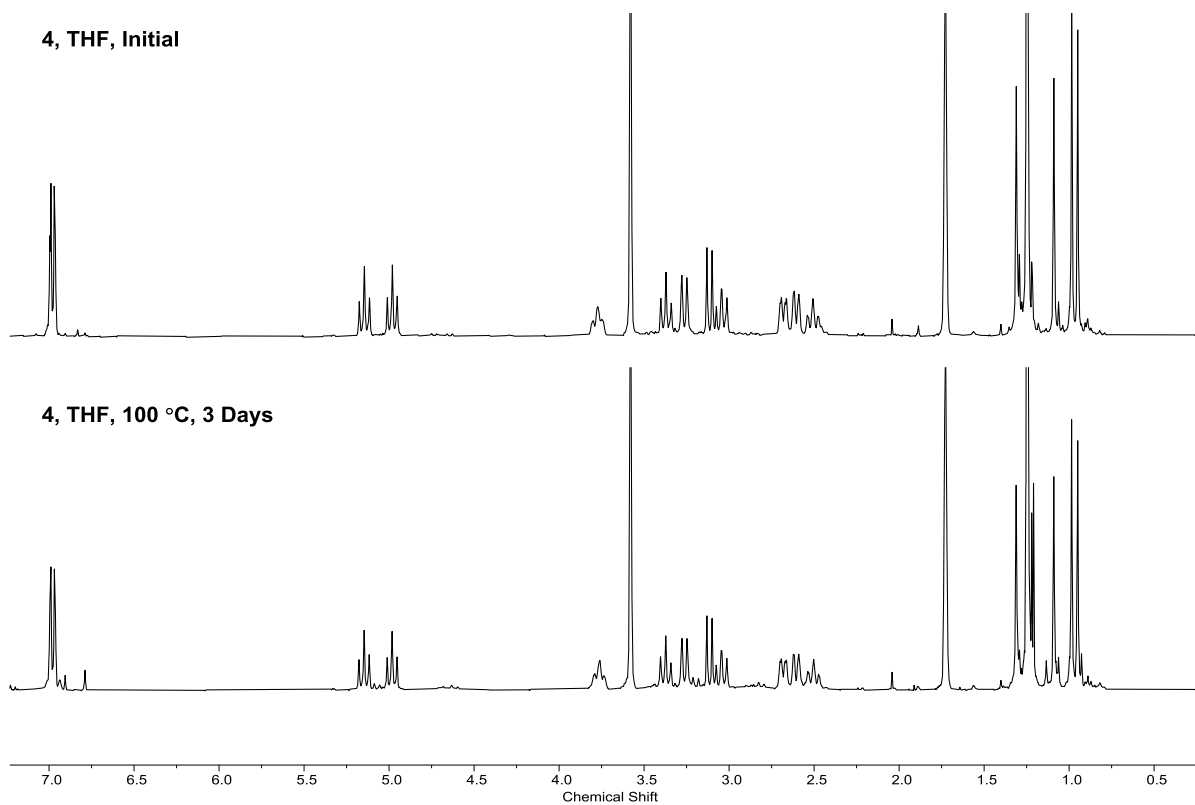


Figure S39: Complex **4** heated to 100 °C in THF for 3 days

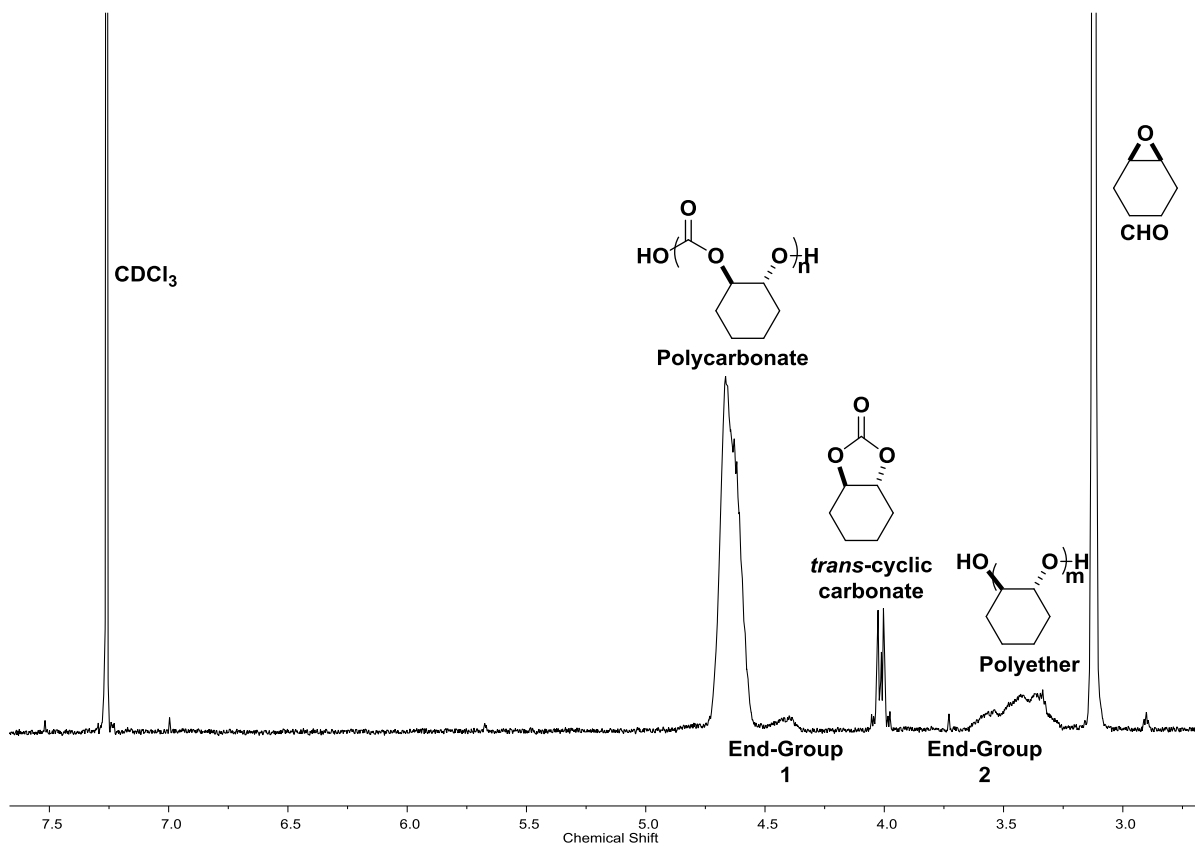


Figure S40: Representative  $^1\text{H}$  NMR of crude polymerisation mixture containing polycarbonate (4.65 ppm) trans-cyclic carbonate (4.00 ppm) and polyether (3.45 ppm) in  $\text{CDCl}_3$  at 298 K.

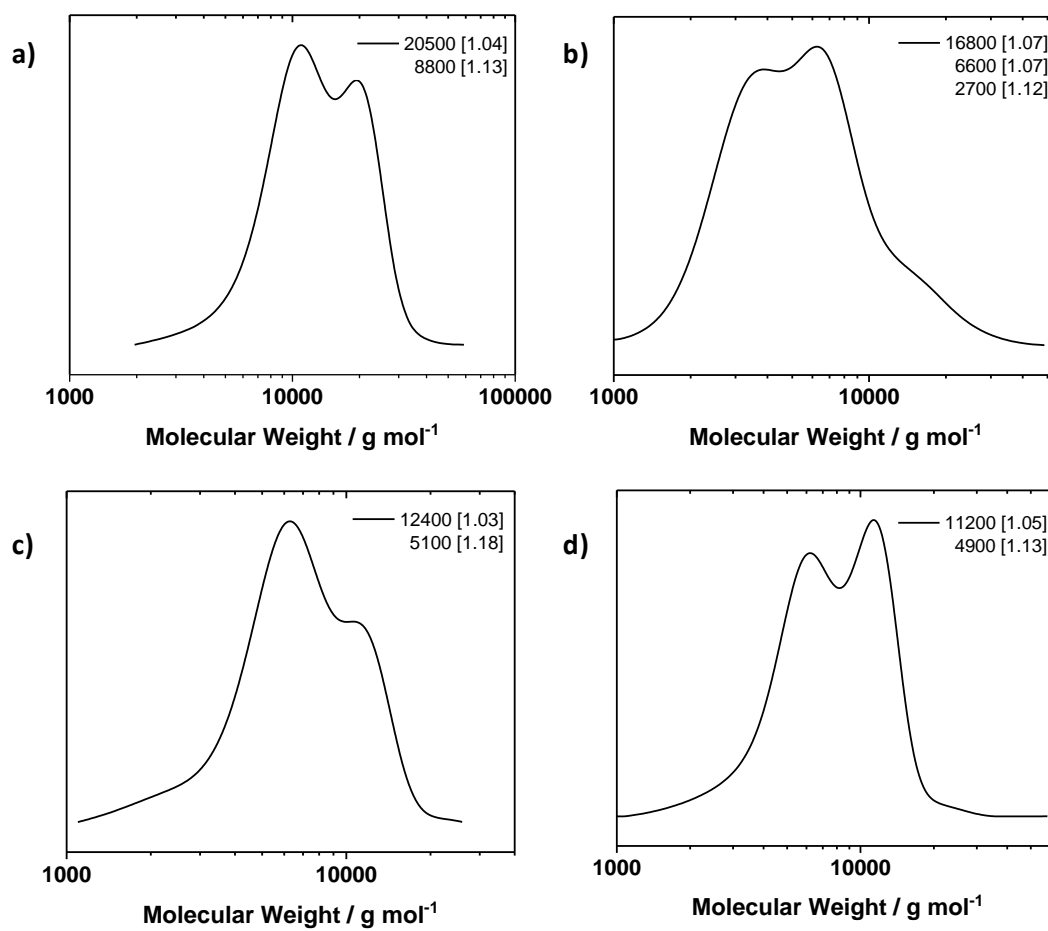


Figure S41: GPC of crude reaction samples reported in Table 1 for a) Entry 1, b) Entry 4, c) Entry 5 and d) Entry 6.

### The X-ray crystal structure of **2**

The Al and Zn in the asymmetric unit are disordered leading to two moieties: Cl1A – Al1 – Cl2 and Zn1 – Cl1B. All five atoms of disorder were found in the difference map and their occupancies constrained to 50%. In addition, it was necessary to apply bond distance restraints to Cl1A – Al1 – Cl2, to ensure a stable refinement. Upon applying the crystallographic C<sub>2</sub> symmetry element to the asymmetric unit, the complete molecule is generated, yielding a Zn/Al heterodimer.

### The X-ray crystal structure of **3**

The Ga and Zn in the asymmetric unit are disordered leading to two moieties: Cl1 – Ga1 – Cl2 and Zn1 – Cl1, with both Zn and Ga sharing a common chloride (Cl1). The disordered atoms were found in the difference map and their occupancies constrained to 50%. Upon applying the crystallographic C<sub>2</sub> symmetry element to the asymmetric unit, the complete molecule is generated, yielding a Zn/Ga heterodimer. In addition to the metal disorder, the ligand *tert*-butyl group was found to be disordered over two locations. Two orientations were identified and their occupancy allowed to refine on a free variable. Bond distances of the disorder were restrained to allow for stable refinement.

### The X-ray crystal structure of **4**

The asymmetric unit of **4** contains the entire Zn/In heterodimer. As in **2** and **3** the In and Zn metals were disordered along with their corresponding chlorides. This disorder can be divided into two parts containing: Zn1 – Cl2 and Cl2 – In1 – Cl1A in one part and Zn2 – Cl3 and Cl3 – In2 – Cl1B. In each case, Zn and In share a common chloride of 100% occupancy, Cl2 in the case of Zn1/In1 and Cl3 in the case of Zn2/In2. Bond distances of the metal disorder were restrained to allow for stable refinement. Both the C41 and C58 *tert*-butyl groups in the **1** were found to be disordered. Two orientations of each were identified and their occupancy allowed to refine on a free variable. In addition, both C7 and C24 *tert*-butyl groups were found to be disordered. Bond distances and thermal parameters of the disorder were restrained to allow for stable refinement. Lastly, highly disordered solvent was found in the crystal lattice which was unable to be sufficiently modeled and the SQUEEZE<sup>1</sup> protocol of the PLATON<sup>2</sup> suite of programs was utilized.

Table S1. Select crystallographic details for **1** – **4**.

Compound	1	2	3	4
Chemical formula	C <sub>36</sub> H <sub>57</sub> Cl <sub>2</sub> N <sub>5</sub> O <sub>2</sub> Zn <sub>2</sub>	C <sub>42</sub> H <sub>66</sub> AlCl <sub>3</sub> N <sub>8</sub> O <sub>2</sub> Zn	C <sub>46</sub> H <sub>72</sub> Cl <sub>3</sub> GaN <sub>10</sub> O <sub>2</sub> Zn	C <sub>34</sub> H <sub>54</sub> Cl <sub>3</sub> InN <sub>4</sub> O <sub>2</sub> Zn
Formula weight	793.50	913.72	1038.57	837.35
Temp (K)	150(2)	150(2)	150(2)	150(2)
Space group	Orthorhombic, <i>Pbca</i>	Monoclinic, <i>I2/a</i>	Orthorhombic, <i>Fddd</i>	Monoclinic, <i>P 2<sub>1</sub>/c</i>
<i>a</i> (Å)	11.9010(1)	12.3857(1)	12.7804(5)	12.9717(4)
<i>b</i> (Å)	24.5866(2)	20.9174(3)	35.8238(12)	12.1675(4)
<i>c</i> (Å)	26.0351(2)	18.7557(2)	47.439(3)	33.7927(12)
$\alpha$ (°)	90	90	90	90
$\beta$ (°)	90	106.889(1)	90	100.382(3)
$\gamma$ (°)	90	90	90	90
<i>V</i> (Å <sup>3</sup> )	7618.00(11)	4649.58(9)	21719.4(17)	5246.3(3)
<i>Z</i>	8	4	16	4
<i>D</i> <sub>calcd</sub> (Mg/m <sup>3</sup> )	1.384	1.305	1.270	1.060
Crystal size (mm)	0.25 X 0.25 X 0.20	0.20 X 0.15 X 0.03	0.20 X 0.20 X 0.05	0.20 X 0.08 X 0.04
Theta range for data collection (°)	3.595 to 76.385	4.227 to 76.128	3.727 to 76.983	3.464 to 76.254
$\mu$ (mm <sup>-1</sup> )	(Cu, K $\alpha$ ) 3.130	(Cu, K $\alpha$ ) 2.842	(Cu, K $\alpha$ ) 2.852	(Cu, K $\alpha$ ) 5.673
Reflections collected	50203	29741	53839	35924
Unique reflections	7927 [R <sub>int</sub> = 0.0283]	4852 [R <sub>int</sub> = 0.0350]	5691 [R <sub>int</sub> = 0.0638]	10899 [R <sub>int</sub> = 0.0676]
Data Completeness to [ $\theta$ ]	100.0% [ 67.684 ]	100.0% [ 67.684 ]	100.0% [ 67.684 ]	100.0% [ 67.684 ]
Data/restraints/parameters	7927 / 0 / 451	4852 / 1 / 295	5691 / 30 / 346	10899 / 320 / 516
R1 [I > 2 $\sigma$ (I)] (all data)	0.0260 (0.0280)	0.0514 (0.0545)	0.0404 (0.0487)	0.0580 (0.0773)
wR2 [I > 2 $\sigma$ (I)] (all data)	0.0674 (0.0688)	0.1068 (0.1080)	0.1056 (0.1124)	0.1289 (0.1376)
Goodness-of-fit on F <sup>2</sup>	1.049	1.266	1.041	1.043
Largest diff. peak and hole (e Å <sup>-3</sup> )	0.398 and -0.466	0.318 and -0.402	0.421 and -0.364	0.901 and -0.666

## References

1. A. Spek, *Acta Crystallographica Section C*, 2015, **71**, 9-18.
2. A. Spek, *Acta Crystallographica Section D*, 2009, **65**, 148-155.